

# Fullerene Derivatives for Tumor Treatment: Mechanisms and Application

Wenjia Hou<sup>1,2,\*</sup>, Lan Shen<sup>1,\*</sup>, Yimin Zhu<sup>1</sup>, Xuanjia Wang<sup>1</sup>, Tianyu Du<sup>1</sup>, Fang Yang<sup>1</sup>, Yabin Zhu<sup>1</sup>

<sup>1</sup>Health Science Center, Ningbo University, Ningbo, 315211, People's Republic of China; <sup>2</sup>State Key Laboratory of Molecular Engineering of Polymers, Fudan University, Shanghai, 200438, People's Republic of China

\*These authors contributed equally to this work

Correspondence: Wenjia Hou; Yabin Zhu, Email houwenjia@nbu.edu.cn; zhuyabin@nbu.edu.cn

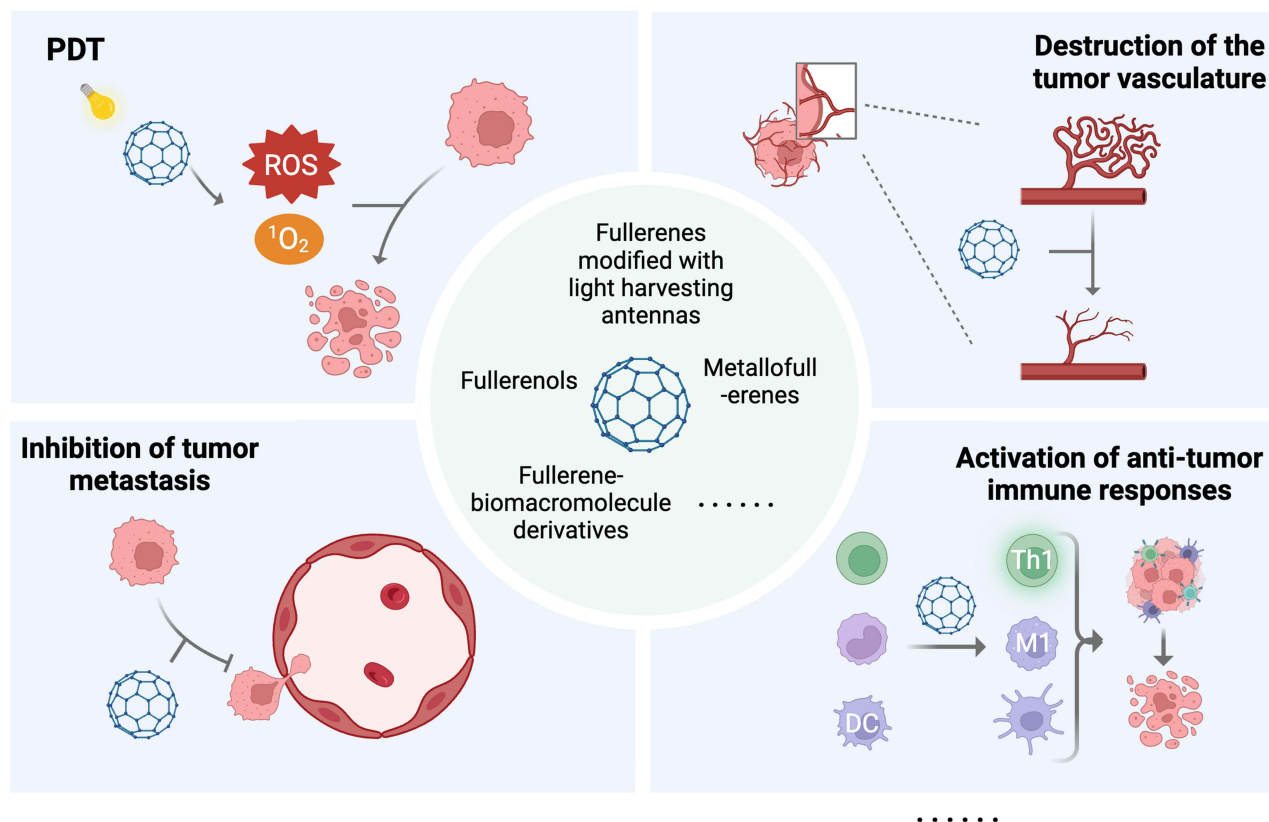
**Abstract:** Fullerenes hold tremendous potential as alternatives to conventional chemotherapy or radiotherapy for tumor treatment due to their abilities to photodynamically kill tumor cells, destroy the tumor vasculature, inhibit tumor metastasis and activate anti-tumor immune responses, while protecting normal tissue through antioxidative effects. The symmetrical hollow molecular structures of fullerenes with abundant C=C bonds allow versatile chemical modification with diverse functional groups, metal clusters and biomacromolecules to synthesize a wide range of fullerene derivatives with increased water solubility, improved biocompatibility, enhanced photodynamic properties and stronger targeting abilities. This review introduces the anti-tumor mechanisms of fullerenes and summarizes the most recent works on the functionalization of fullerenes and the application of fullerene derivatives in tumor treatment. This review aims to serve as a valuable reference for further development and clinical application of anti-tumor fullerene derivatives.

**Keywords:** fullerene derivatives, tumor treatment, photodynamic treatment, metastasis inhibition, tumor vasculature, cellular immunity

## Introduction

Cancer is a highly lethal disease that is notoriously difficult to treat due to its drug resistance and metastasis-proneness. The effectiveness of conventional approaches such as chemotherapy, radiotherapy and surgery is limited by their low efficacy, severe side effects and poor targetability. In recent years, a wide variety of novel tumor treatment approaches<sup>1-5</sup> (eg gene therapy,<sup>2</sup> tumor organoid therapy,<sup>3</sup> exosome therapy<sup>4</sup>) have emerged, among which nanoparticles are promising alternatives to conventional tumor treatment approaches with the advantages of higher targetability, capability of regulating tumor microenvironment, strong tissue penetration abilities, etc.<sup>5,6</sup> Among the nanoparticles applied to tumor treatment, fullerenes, a family of carbon allotropes, have obtained considerable research attention.<sup>7,8</sup> The most representative member of the fullerene family is C<sub>60</sub> composed of 60 carbon atoms with C<sub>5</sub>-C<sub>5</sub> single bonds forming 12 pentagons and C<sub>5</sub>-C<sub>6</sub> double bonds forming 20 hexagons, forming a highly symmetrical cage-like structure.<sup>9,10</sup> In fact, fullerenes encompass a larger family, including C<sub>70</sub>, C<sub>84</sub> and others, which are typically formed by the addition of one or more hexagonal rings to the C<sub>60</sub> framework.<sup>11</sup> The abundant C=C bonds on the surface of fullerenes pave the way for versatile chemical modification with diverse functional groups and metal ions to synthesize a wide range of fullerene derivatives such as metallofullerenes, fullerlenols and fullerene biomacromolecules.<sup>12-14</sup> Under light irradiation, fullerene derivatives are capable of generating reactive oxygen species (ROS) that can effectively kill tumor cells, establishing the basis for the photodynamic treatment (PDT) of cancer.<sup>15,16</sup> Fullerene derivatives can also destroy the tumor vasculature, depriving tumors of their nutrient supply to starve tumor cells.<sup>17-19</sup> Additionally, fullerene derivatives are capable of inducing the formation of dense fibrous “prisons” to confine tumors, inhibiting tumor infiltration and metastasis.<sup>20</sup> Moreover, fullerene derivatives can regulate the secretion of certain biomacromolecules to the extracellular matrix to regulate the tumor microenvironment, inhibit tumor growth and suppress metastasis.<sup>21</sup>

## Graphical Abstract



Fullerenes are also recognized for their ability to effectively scavenge free radicals due to the presence of numerous conjugated double  $\pi$  bonds with low energy unoccupied molecular orbitals, enabling them to readily accept an electron and engage in reactions with radical species.<sup>22,23</sup> Consequently, fullerenes are often referred to as “radical sponge” due to their capacity to scavenge free radicals and provide protection for normal tissue during chemotherapy and radiotherapy.<sup>24</sup> Therefore, fullerenes hold tremendous potential in tumor treatment and are worth further exploration and utilization. This review aims to comprehensively summarize the anti-tumor mechanisms of fullerenes and recent advances in the construction of anti-tumor fullerene derivatives.

## Anti-Tumor Mechanisms of Fullerenes

### Photodynamic Treatment

PDT is an emerging method for tumor treatment based on the photoactivation of photosensitizers (PS) accumulated at the tumor site by irradiation of light of specific wavelengths and the resulting generation of ROS to damage tumor cells.<sup>25–27</sup>

Compared to conventional cancer therapy such as chemotherapy and radiotherapy, PDT offers several advantages including higher targetability, lower toxicity, minimal invasiveness and lower long-term recurrence rate.<sup>26,28</sup> Furthermore, the different distribution of cell surface receptors as well as the increased metabolic activities of tumor cells compared to normal cells result in targeted accumulation of ROS produced by PDT within tumor cells, thereby improving treatment efficacy.<sup>29</sup> PDT has been increasingly employed in the treatment of various types of cancer, eg skin cancer, gastrointestinal cancer, lung cancer, etc.<sup>30</sup> In the process of PDT, PS is the determining factor of photodynamic efficacy. The ideal PS should have good photostability, high triplet state yields, high targetability and low toxicity to normal tissue.<sup>30,31</sup>

Fullerenes, with their high triplet state conversion rates (~100%), high ROS yields, good photostability, and ability to undergo versatile functionalization, can serve as excellent PS for PDT.<sup>15,32,33</sup> When exposed to ultraviolet (UV) or visible light, fullerenes can be excited into a transient singlet state, which rapidly transforms into the triplet state, resulting in the production of abundant ROS and singlet oxygen ( $^1\text{O}_2$ ).<sup>26,28,34</sup> This process can promote the oxidation of biomacromolecules, peroxidation of lipids and photooxidation of DNA guanine base components, causing damage to the cell membrane and cytoskeleton, and ultimately leading to cell death.<sup>23</sup> The possible mechanisms underlying the photodynamic killing of tumor cells by fullerenes can be classified into mitochondria-induced cell apoptosis and cell membrane disruption-induced cell death.

### Mitochondria-Induced Cell Apoptosis

Previous research has indicated that upon uptake by tumor cells, fullerenes tend to aggregate in mitochondria, where the photodynamically-produced ROS can result in mitochondrial dysfunction and ultimately induce cell apoptosis through the mitochondrial pathway.<sup>33–38</sup> Once inside tumor cells, ROS can lead to alterations in the electron transport chain located on the inner mitochondrial membrane, causing a loss of potential difference and an increase in mitochondrial membrane permeability.<sup>35,39,40</sup> Cells undergoing apoptosis through the mitochondrial pathway exhibit characteristic features such as the release of pro-apoptotic factors including inhibitor of apoptosis protein, P53 and the B-cell lymphoma-2 family from the mitochondria into the cytoplasm.<sup>39,41</sup> This process promotes the formation of the apoptosome, initiating a cascade reaction involving Caspases through the recruitment and activation of Pro-Caspase 9. As a result, more than 100 substrates in cells, including inhibitor of caspase-activated DNase, poly ADP-ribose polymerase and Lamin, are cleaved, ultimately leading to cell apoptosis.<sup>39,41–43</sup> Mroz et al characterized the Caspase activities of colon cancer cells CT26 during fullerene-based PDT, and found that the Caspase activities started to increase as early as the 2nd hour of irradiation, peaked at the 4th–6th hour, and then decreased after 12 hours, providing evidence that fullerenes induced tumor cell apoptosis by compromising mitochondria.<sup>44</sup>

Another notable characteristic of apoptosis is DNA degradation.<sup>45</sup> With the alteration in mitochondrial membrane potential, apoptosis factors such as endonuclease G and apoptosis-inducing factor are released and translocated into the nucleus,<sup>46</sup> resulting in chromosome condensation, DNA fragmentation, and ultimately cell apoptosis.<sup>39</sup> Shi and colleagues used agarose gel electrophoresis to analyze the impact of a fullerene derivative diadduct malonic acid-fullerene-Asn-Gly-Arg peptide (DMA-C<sub>60</sub>-NGR) on the DNA of MCF-7 tumor cells under light irradiation. The results revealed that at a concentration as low as 5  $\mu\text{g}/\text{mL}$ , DMA-C<sub>60</sub>-NGR significantly induced nuclear DNA fragmentation in tumor cells, ultimately leading to apoptosis.<sup>38</sup>

### Cell Membrane Disruption-Induced Cell Necrosis

This type of cell death, known as cell necrosis, is characterized by cytoplasmic vacuolation, plasma membrane breakdown and release of cellular contents, leading to inflammatory responses. Fullerenes are capable of photodynamically generating large amounts of ROS, resulting in rapid lipid peroxidation and increased cell membrane permeability.<sup>47,48</sup> When comparing the photocytotoxicity of a dendritic C<sub>60</sub> mono-adduct and a malonic acid C<sub>60</sub> tris-adduct towards tumor cells, Rancan et al noticed that the malonic acid C<sub>60</sub> tris-adduct with lower  $^1\text{O}_2$  yields demonstrated stronger cytotoxicity, indicating that the sheer volume of  $^1\text{O}_2$  is not the only factor affecting anti-tumor effectiveness. The authors attributed this seemingly illogical phenomenon to the difference in the molecular structures of the two fullerene derivatives, which resulted in the different patterns of their interaction with the tumor cell membrane. The malonic acid C<sub>60</sub> tris-adducts were uniformly adsorbed on the cell membrane, causing more efficient cell membrane disruption, while the branches of the dendritic C<sub>60</sub> mono-adducts kept them further away from tumor cells, hampering their contact with the cell membrane.<sup>40</sup> Furthermore, Kamat et al reported that the free radicals photodynamically generated by fullerenes caused damage not only to membrane-binding enzymes, but also to oxidative proteins, ultimately leading to cell necrosis.<sup>49</sup> Figure 1 depicts the two mechanisms of the photodynamic killing of tumor cells by fullerene derivatives.

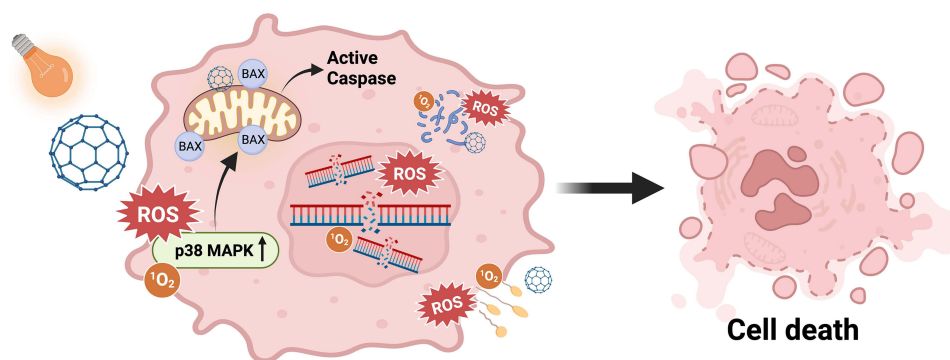


**Figure 1** Schematic diagrams of the anti-tumor mechanisms of fullerene-based PDT. Fullerenes generate ROS and  $^1\text{O}_2$  through a photodynamic process, inducing apoptosis and necrosis in cells. Apoptosis is primarily caused by the accumulation of fullerenes in the mitochondria, which leads to the disruption of the electron transport chain and degradation of DNA. Necrosis is mainly caused by the peroxidation of biomacromolecules such as proteins and membrane lipids. Created in BioRender. Yang, F. (2024) BioRender.com/x74o589.

## Inhibition of Tumor Metastasis

Fullerene derivatives have been reported to exhibit inhibitory effects on the metastasis of cancer, which accounts for the majority of cancer mortality,<sup>10</sup> especially for highly invasive and metastatic cancers such as lung cancer, breast cancer and colorectal cancer.<sup>50</sup> The mechanisms of such metastasis inhibition can be categorized as follows: I. Fullerenes disrupt the formation of the cytoskeleton of tumor cells (which is the basis of their motility) by impairing the self-assembly of actin (a major constituent of the cytoskeleton) and altering the distribution of key proteins (eg integrin) regulating intercellular contact, thereby reducing the migration activities of tumor cells.<sup>51</sup> II. Fullerenes promote the formation of dense extracellular matrices (ECM) (especially fibrous “cages” formed by collagen), enwrapping tumor tissue to prevent metastasis.<sup>20</sup> Normally, tumor cells and adjacent cells (eg recruited tumor-associated macrophages (TAMs)) secrete abundant matrix metalloproteinases (MMPs) that cause the degradation of the ECM, forming escape channels to pave the way for tumor metastasis.<sup>52–54</sup> Fullerenes can effectively inhibit MMP secretion and reduce MMP activities, while promoting collagen secretion and increasing collagen stability to form dense fibrous “cages” confining tumor cells.<sup>55</sup> III. Fullerenes can also inhibit tumor metastasis by affecting the interactions between tumor cells and mesenchymal stem cells.<sup>56</sup> Tumor development is usually associated with the recruitment of various stromal cells with potential tumor-promotive activities, among which mesenchymal stem cells, an important type of stromal progenitor cells with multipotent differentiation potential, play a crucial role in tumorigenesis.<sup>57</sup> The interactions between tumor cells and mesenchymal stem cells greatly promote tumor development and metastasis. Tumor cells can induce the malignant differentiation of mesenchymal stem cells, eg into cancer-associated fibroblasts.<sup>58</sup> On the other hand, mesenchymal stem cells can promote tumor growth and metastasis.<sup>57</sup> Fullerenes have been reported to block the interaction between breast cancer cells and marrow-derived mesenchymal stem cells by regulating signaling pathways such as nuclear factor-KB (NF-KB).<sup>56</sup> Furthermore, fullerenes can inhibit tumor metastasis by reversing the epithelial-mesenchymal transition (EMT), the emblem of the initiation of tumor metastasis. EMT is the process in which epithelial cells gradually lose polarity and intercellular contact and transform into mesenchymal cells,<sup>59</sup> and is a main contributing factor of tumor metastasis.<sup>60,61</sup> During tumor development, the occurrence of EMT increases the invasion and metastatic potential of tumor cells, facilitating their entry into surrounding tissues and blood vessels for distant metastasis.<sup>62</sup> Fullerene derivatives can bind to certain EMT-regulating proteins to reverse the EMT process and inhibit tumor cell migration.<sup>63</sup> Horak et al used 10  $\mu\text{M}$  C<sub>60</sub>-Ber nanocomplexes to modulate the levels of epithelial and mesenchymal markers in Lewis lung carcinoma cells (LLC), and found that down-regulating the levels of EMT-inducing transcription factors SNAI1, ZEB1 and TWIST1 significantly increased E-cadherin expression and reduced Ruk/CIN85 levels, inducing a mesenchymal-to-epithelial transition in LLC, indicating the ability of C<sub>60</sub>-Ber to reverse the EMT process and inhibit LLC cell migration.<sup>64–66</sup> Furthermore, fullerene derivatives can reverse EMT by compromising the cytoskeleton. Myosin heavy chain 9, a cytoplasm-located protein responsible for cell motility and EMT regulation, is overexpressed in various cancers and contributes to metastasis. Zhou et al reported that an aminated fullerene derivative C<sub>70</sub>-EDA bound to the C terminal of myosin heavy chain 9 through electrostatic interactions, occupying the binding sites regulating

cytoskeleton assembly at the C terminal, thereby decreasing tumor cell motility. C<sub>70</sub>-EDA with a concentration of 10 μM effectively inhibited the metastasis of various cancers without causing tumor cell apoptosis. An increase of the epithelial marker E-cadherin and a reduction of mesenchymal markers (vimentin and N-cadherin) were observed after C<sub>70</sub>-EDA administration, indicating the successful reversal of EMT.<sup>63</sup> Currently, research on the use of fullerene derivatives to inhibit the EMT process is limited, and further studies are needed to verify the efficacy of this strategy. The three mechanisms of the metastasis inhibition by fullerenes are schematically described in Figure 2.

## Destruction of the Tumor Vasculature

Being a fundamental process in tumor development, tumor angiogenesis provides necessary nutrients for tumor growth and metastasis.<sup>67,68</sup> It is widely recognized that the oxygen-deficient environment in tumor tissue affects the effectiveness of PDT (which requires oxygen to produce ROS and <sup>1</sup>O<sub>2</sub>).<sup>69</sup> Nevertheless, the abundant oxygen in the tumor vasculature provides “fuel” for fullerene derivatives to produce ROS and <sup>1</sup>O<sub>2</sub> under irradiation,<sup>70</sup> rendering the tumor vasculature vulnerable to PDT. ROS and <sup>1</sup>O<sub>2</sub> can inactivate the endothelial cells of the tumor vasculature, cutting off the tumor tissue

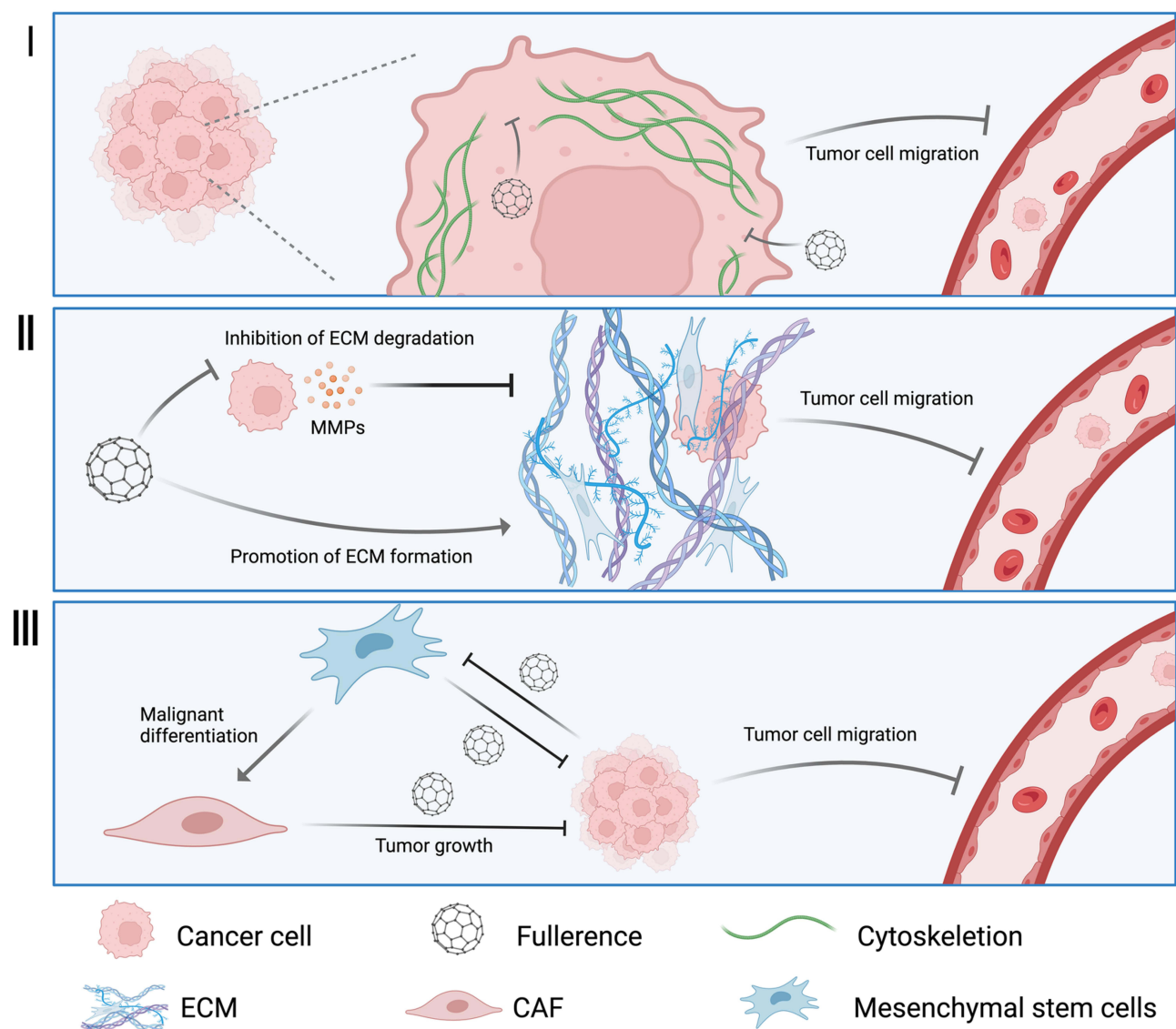


**Figure 2** Schematic diagrams of the metastasis inhibition by fullerenes. I: Fullerenes disrupt the self-assembly of the cytoskeleton, thereby inhibiting tumor cell migration. II: Fullerenes inhibit MMP secretion and promote dense ECM formation, enveloping tumor cells to prevent migration. III: Fullerenes block tumor cell-mesenchymal stem cell interactions and reverse the EMT process, thereby inhibiting tumor metastasis. Created in BioRender. Yang, F. (2024) BioRender.com/x74o589.

from nutrient supply and eventually starving tumor cells.<sup>71</sup> Moreover, the tumor vasculature is susceptible to attacks due to its loose and highly permeable structure, consisting only of monolayer endothelial cells without complete basement membranes.<sup>72,73</sup> Fullerene derivatives (especially metallofullerenes) can infiltrate into the gaps in the tumor vasculature structure and destroy tumor blood vessels. It was reported that when injected intravenously into mice, metallofullerenes underwent phase transformation and acute size expansion at the gaps in the tumor vasculature under radio frequency (RF) irradiation, physically disrupting and detaching endothelial cells, thereby depriving the tumor of its nutrient supply. Importantly, normal blood vessels and organs were unaffected due to their relatively intact and less permeable structures.<sup>17,18</sup>

## Activation of Anti-Tumor Immune Responses

Apart from acting directly on tumor cells, fullerene derivatives can attack tumors by activating cellular immunity. Prylutska et al observed that a C<sub>60</sub>-Cis-Pt nanocomposite induced significant infiltration of inflammatory cells into the tumor tissue in mice, suggesting that the nanocomposite might have activated cellular immunity as one of its anti-tumor mechanisms.<sup>74</sup> Chen et al reported that when [Gd@C<sub>82</sub>(OH)<sub>22</sub>]<sub>n</sub> was administered to mice at a low dosage (10<sup>-7</sup> mol/kg), despite the lack of noticeable cytotoxicity to tumor cells in vitro, only 0.05% of the administration dosage reaching the tumor tissue exhibited desirable anti-tumor effects by activating cellular immunity.<sup>75</sup> Recent studies have shed light on the mechanisms of the immunostimulatory properties of fullerene derivatives.<sup>76-78</sup> Tumor cells typically have strategies to evade the surveillance and elimination by the immune system in order to grow and migrate “off the radar”. Tumor immunotherapy is a strategy aiming to awaken the immune system and restore normal anti-tumor immune responses.<sup>79</sup> Mature dendritic cells (DCs) play a crucial role in tumor immunotherapy by facilitating antigen presentation, T cell activation and immunomodulation to promote the recognition and targeting of tumor cells by the immune system.<sup>80-82</sup> Upon receiving antigenic and co-stimulatory signals from mature DCs, T cells are activated and differentiate into Th1 cells, secreting cytokines such as interleukin-12 (IL-12) and interferon- $\gamma$  (IFN- $\gamma$ ) to recruit other immune cells, thereby activating immune attacks to tumor cells, promoting immune cell infiltration into tumor tissue and inhibiting tumor angiogenesis.<sup>83</sup> Fullerene derivatives can effectively promote the maturation of DCs and differentiation of T cells into Th1 cells, resulting in immune cell infiltration.<sup>84</sup> Moreover, TAMs also play a critical role in tumor growth, invasion and metastasis. TAMs have two distinct phenotypes: M1 macrophages with anti-tumor properties and M2 macrophages that support tumor progression.<sup>85</sup> Generally, the majority of TAMs are M2 macrophages that contribute to tumor development, immunosuppression and inhibition of intratumor immune responses.<sup>86,87</sup> Therefore, a promising strategy in cancer immunotherapy is to switch the phenotype of TAMs from M2 to M1. By regulating relevant tumor-associated signaling pathways, fullerene derivatives can promote the differentiation of macrophages towards the M1 phenotype and M2-to-M1 transition of TAMs, as well as subsequent secretion of cell factors such as tumor necrosis factor (TNF- $\alpha$ ) and IFN- $\gamma$ , inducing tumor cell apoptosis. Furthermore, fullerene derivatives can facilitate the phagocytosis of tumor cells by the immune system by triggering the expression of tumor-associated antigens (TAAs, eg calreticulin (CRT)) on the surface of tumor cells, resulting in phagocyte-mediated programmed cell removal.<sup>88,89</sup> The mechanisms of the anti-tumor immune response activation by fullerenes are schematically described in Figure 3.

## Common Fullerene Derivatives and Their Application in Anti-Tumor Treatment

Anti-tumor application of pure fullerenes, however, is severely limited by certain inherent drawbacks of fullerenes, eg poor water solubility and short adsorption range. Functionalization of the fullerene surface with various groups to produce fullerene derivatives is a promising strategy to fully exploit their anti-tumor potential. The abundant C=C bonds on the surface of fullerenes pave the way for versatile chemical modification with diverse functional groups, metal clusters and biomacromolecules to synthesize a wide range of fullerene derivatives such as metallofullerenes, fullerlenols and fullerene-biomacromolecule derivatives with increased water solubility, improved biocompatibility, enhanced photodynamic properties, stronger targeting abilities, etc. This section provides a detailed introduction to the application of commonly used fullerene derivatives in tumor treatment. Table 1 summarizes common fullerene derivatives and their applications in anti-tumor therapy.

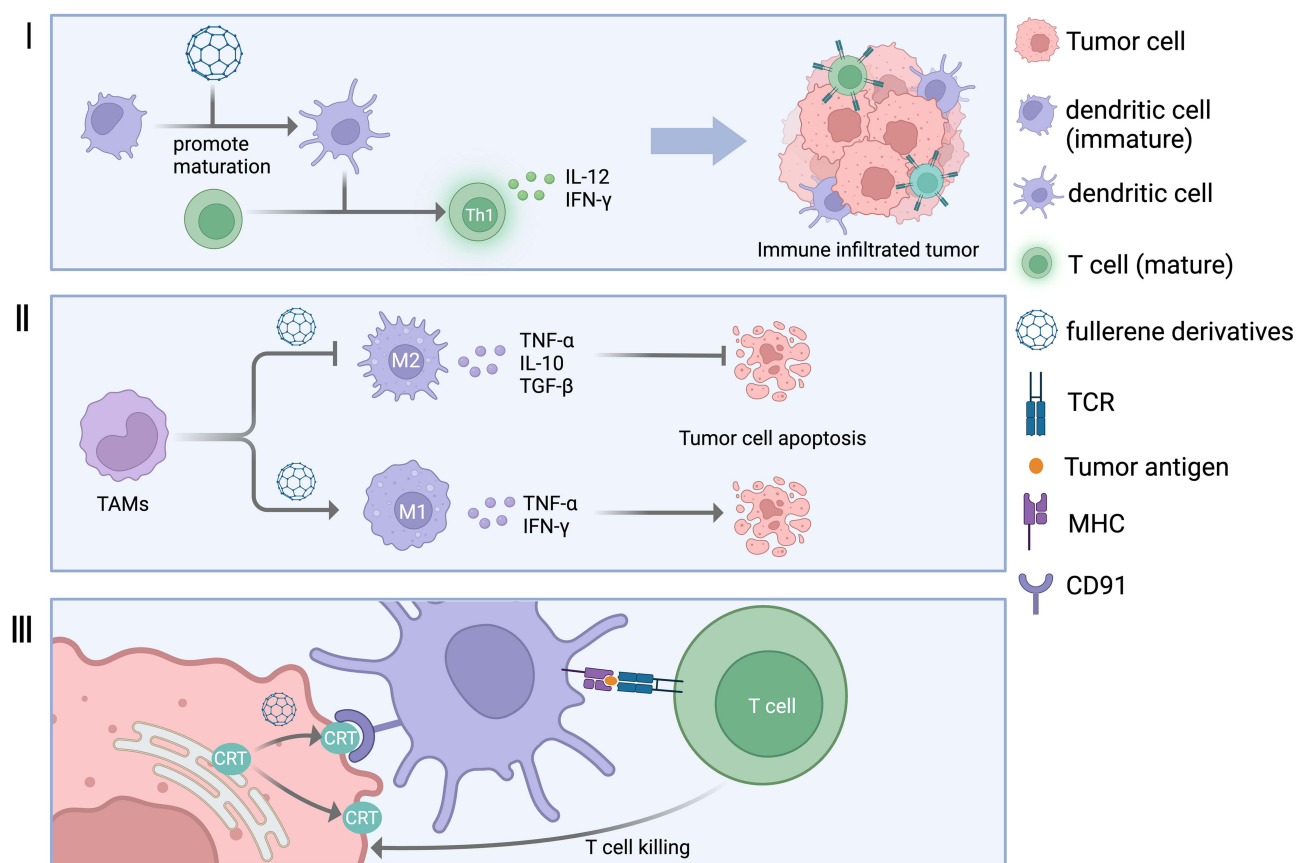


**Figure 3** Schematic diagrams of the anti-tumor immune response activation by fullerenes. I: Fullerenes promote the maturation of DCs and differentiation of T cells into Th1 cells, resulting in immune cell infiltration. II: Fullerenes promote the differentiation of macrophages towards the M1 phenotype and the M2-to-M1 transition of TAMs. III: Fullerenes facilitate the phagocytosis of tumor cells by increasing the expression of CRT on the cell surface, resulting in phagocyte-mediated programmed cell removal. Created in BioRender. Yang, F. (2024) BioRender.com/x74o589.

## Fullerenes Modified with Light-Harvesting Antennas

The use of fullerenes as PS for PDT in deep-seated tumors is limited by their short absorption wavelengths, which are typically in the green, blue, or UV range, making it difficult for light to penetrate deep into the body.<sup>112,113</sup> Near-infrared (NIR) light, with a wavelength of approximately 700–1100 nm, has been identified as an ideal light source for treating deep-seated tumors.<sup>114,115</sup> Therefore, fullerene-based hybrid materials with NIR-adsorption abilities have been developed to enhance the effectiveness of PDT.

Li et al created a hybrid material consisting of oxidized graphene and C<sub>60</sub> (GO-C<sub>60</sub>) (Figure 4A), where the excited state energy of the graphene oxide is directly transferred to the ground state C<sub>60</sub>, enabling light absorption in the NIR region instead of in the green region.<sup>16</sup> Chiang et al synthesized a photoresponsive C<sub>60</sub>-DCE-diphenylaminofluorene nanomolecule, C<sub>60</sub> (>CPAF-Cn) (Figure 4B), with an excitation wavelength of 1000–1200 nm. This nanomolecule achieved efficient killing of HeLa cells in vitro under white light irradiation,<sup>90</sup> however, there is currently no experimental evidence demonstrating their efficacy in killing tumors in vivo.

Upconversion fluorescent nanoparticles (UCNPs) have also been employed as light-harvesting antennas for antitumor PDT,<sup>116</sup> converting NIR light to visible light and facilitating energy transfer to PS for increased tissue penetration depths.<sup>117</sup> Liu et al developed an NIR-excited PDT system based on multi-resonance energy transfer, utilizing lanthanide-doped UCNPs as the electron donor and mono-acrylic fullerene C<sub>60</sub>MA as the electron acceptor. This system enables deep-tissue imaging and high-contrast NIR luminescence.<sup>91</sup> Effective killing of HeLa cells was observed under low-intensity NIR light irradiation, with the effect proportional to the system's concentration. Du et al loaded C<sub>60</sub>, Fe<sub>3</sub>O<sub>4</sub> nanoparticles, UCNPs and a chemotherapy drug docetaxel (DTX) into N-succinyl-N'-4-(2-nitrobenzyloxy)-succinyl chitosan (SNSC) micelles (Figure 4C). The anti-tumor

**Table 1** Common Fullerene Derivatives for Anti-Tumor Applications

Fullerene Derivative	Function	Mechanism	Effect	Reference
GO-C <sub>60</sub>	PS for PDT	The excited state energy of the graphene oxide is directly transferred to the ground state C <sub>60</sub> , enabling light absorption in the NIR region instead of in the green region.	Effective in killing HeLa cells.	[16]
C60(>CPAF-Cn)	PS for PDT	Through chemical conversion of the keto group in C60(>DPAF-Cn) to a strong electron-withdrawing DCE subunit, extend excitation wavelength to 1000–1200 nm.	Effective in killing HeLa cells in vitro.	[90]
Lanthanide-doped UCNP-C <sub>60</sub> MA	PS for PDT	Using lanthanide-doped UCNPs as the electron donor and mono-acrylic fullerene C <sub>60</sub> MA as the electron acceptor; extend excitation wavelength to the NIR region (~980 nm).	Effective killing of HeLa cells under low-intensity NIR light irradiation; deep tissue imaging and high-contrast NIR luminescence.	[91]
C <sub>60</sub> /Fe <sub>3</sub> O <sub>4</sub> -UCNPs@DTX@SNSC	PS for PDT	Under 980 nm excitation, the conversion of NIR to UV, and NIR to visible light can be achieved, and the fullerene can be excited to release a large number of ROS.	Synergistic killing of tumor cells by targeted release of chemotherapy drugs and PDT.	[92]
DAF	PS for PDT and PTT	By conjugating NIR-absorbing antenna with fullerenes, shift the absorption wavelength from 532 nm (green region) to 720 nm (NIR region).	Increased penetration abilities and retainability of DAF NPs led to their accumulation around the tumor site, enabling synergistic PDT and PTT against HeLa cells in vivo.	[93]
Fullerenols C <sub>60</sub> (OH) <sub>n</sub> (n= 18–22)	PS for PDT	Induce cell apoptosis through the mitochondrial pathway and cell cycle arrest at the G2 phase by photodynamic production of ROS.	Inhibited the growth of leukemia cells at high concentrations but promoted tumor cell growth at low concentrations.	[94]
Fullerenol nanoparticles	Tumor metastasis inhibition	Inhibit tumor cell migration by interfering with the physiological balance of G-actin and F-actin.	Decreased the ability of MCF-7 breast cancer cells to pass through blood vessels and further metastasis to the lungs.	[51]
Fullerenol C <sub>60</sub> (OH) <sub>20</sub>	Tumor metastasis inhibition	Reduce tumor vascular density and impair the nutritional supply to tumor cells.	Exhibited in vivo anti-tumor and anti-metastasis activities in the EMT-6 breast cancer metastasis model, with no direct in vitro cytotoxicity towards breast cancer cells.	[95]
C <sub>60</sub> (OH) <sub>22</sub> nanoparticles	Tumor metastasis inhibition	Decrease the secretion of key cell factors for malignant progression of BDMSCs by regulating the MAPK signaling pathway, thereby weakening the cascade between BDMSCs and 4T1 breast cancer cells.	Inhibited the promotional effect of BDMSCs on tumor metastasis, with minimal side effects on normal tissue.	[56]
C <sub>60</sub> (OH) <sub>24</sub>	Protective agent in radiotherapy	Protect normal tissue from oxidative damage by scavenging ROS produced during radiotherapy.	Exhibited a superior protective effect on the spleen, the small intestines and the lungs against X-ray radiation than the commonly used radioprotective drug amifostine; reduced whole body irradiation-induced mortality without noticeable toxicity.	[96,97]
Ful-Dox	Protective agent in chemotherapy	Protect normal tissue from oxidative damage by scavenging ROS produced by chemotherapy drugs.	Effectively reduced the systemic toxicity of DOX on the brain, eye, spleen and the cardiovascular system.	[98–100]



FNPs	Activation of anti-tumor immune responses	Induce stress responses of the endoplasmic reticulum, triggering CRT exposure on tumor cells and effectively promoting programmed tumor cell clearance by phagocytes.	When used with half-dose anti-CD47 mAb, FNPs achieved similar effectiveness in treating subcutaneous glioblastoma U87MG and in situ osteosarcoma 143B to using full-dose anti-CD47 mAb alone.	[88]
Gd@C <sub>82</sub> (OH) <sub>22</sub>	Tumor metastasis inhibition Activation of anti-tumor immune responses	Reduce MMP production and activities while promoting Collagen Type I & III formation, forming dense collagen microfibers around tumors to inhibit metastasis. Promote DC maturation and T cell differentiation towards the Th1 phenotype. Bind to complement C1q, enhancing activation of the complement cascade.	The thickness of the fibrous enclosure in the presence of Gd@C <sub>82</sub> (OH) <sub>22</sub> increased to more than five-folds that of the control group. No cytotoxicity to normal cells. The antigen-specific Th1 immune response of tumor-bearing mice was enhanced, and a large number of white blood cells were infiltrated in residual tumor tissue Bound to a significant amount of C1q in the serum of human lung squamous cell carcinoma patients, activating the immune system.	[20,55,101–104] [84] [105]
Gd-Ala	PS for V-PDT	Destroy tumor vascular endothelial cells by photodynamic production of ROS.	Hemorrhage was observed at the periphery of the tumor vasculature 20 min after the start of V-PDT and continued for another 40 min. Segments of tumor vessels then began to collapse with severe hemorrhage.	[71]
β-alanine modified GFNPs	Activation of anti-tumor immune responses PS for PDT	Promote DCs maturation, activating the cytotoxic activity of CD8 <sup>+</sup> T lymphocytes. Destroy VE-cadherin and reduce the secretion of CD31 by tumor vascular endothelial cells, inducing rapid tumor necrosis.	Three days after V-PDT treatment, the levels of CD4 <sup>+</sup> and CD8 <sup>+</sup> T lymphocytes significantly increased. By the 7th day, there was a notable rise in TNF-α secretion. The anti-tumor effectiveness of the GFNPs was found to be correlated to particle size, as smaller GFNPs exhibited the highest efficiency.	[71] [106]
GFNCs	Destruction of the tumor vasculature	Enter the gaps between endothelial cells and destroy the tumor blood vessel endothelium by size expansion during phase change under RF irradiation.	Led to tumor necrosis and detachment.	[18]
Gd@C <sub>82</sub> (GF-Ala)	Activation of anti-tumor immune responses	Induce an M2 to M1 phenotype transition of TAMs; increase the infiltration of CTLs into tumor tissue.	Using GF-Ala nanoparticles with anti-tumor drug anti-PD-L1 immune checkpoint inhibitor achieved a superior synergistic treatment effect.	[89]
C <sub>60</sub> -phe, C <sub>60</sub> -gly	PS for PDT	Produce abundant ROS through type II mechanism to inhibit cell division, induce DNA cleavage and cell apoptosis.	Caused the apoptosis of human liver cancer cells SMMC-7721 under white light irradiation, with no cytotoxicity in the dark.	[107]
Val-C <sub>60</sub> , Ala-C <sub>60</sub> and Pro-C <sub>60</sub>	PS for PDT	Photodynamic mechanism shifted from type II ( <sup>1</sup> O <sub>2</sub> generation) to type I (superoxide generation), improving PDT effectiveness in hypoxic environments.	Exhibited pronounced phototoxicity on HeLa cells.	[108]
Sweet-C <sub>60</sub>	PS for PDT; glucose baits for highly glucose-dependent tumors	Strong affinity with glucose receptors, facilitating its uptake by highly glucose-dependent tumor cells.	Increased the uptake by highly glucose-dependent tumors, particularly pancreatic ductal adenocarcinoma.	[109–111]

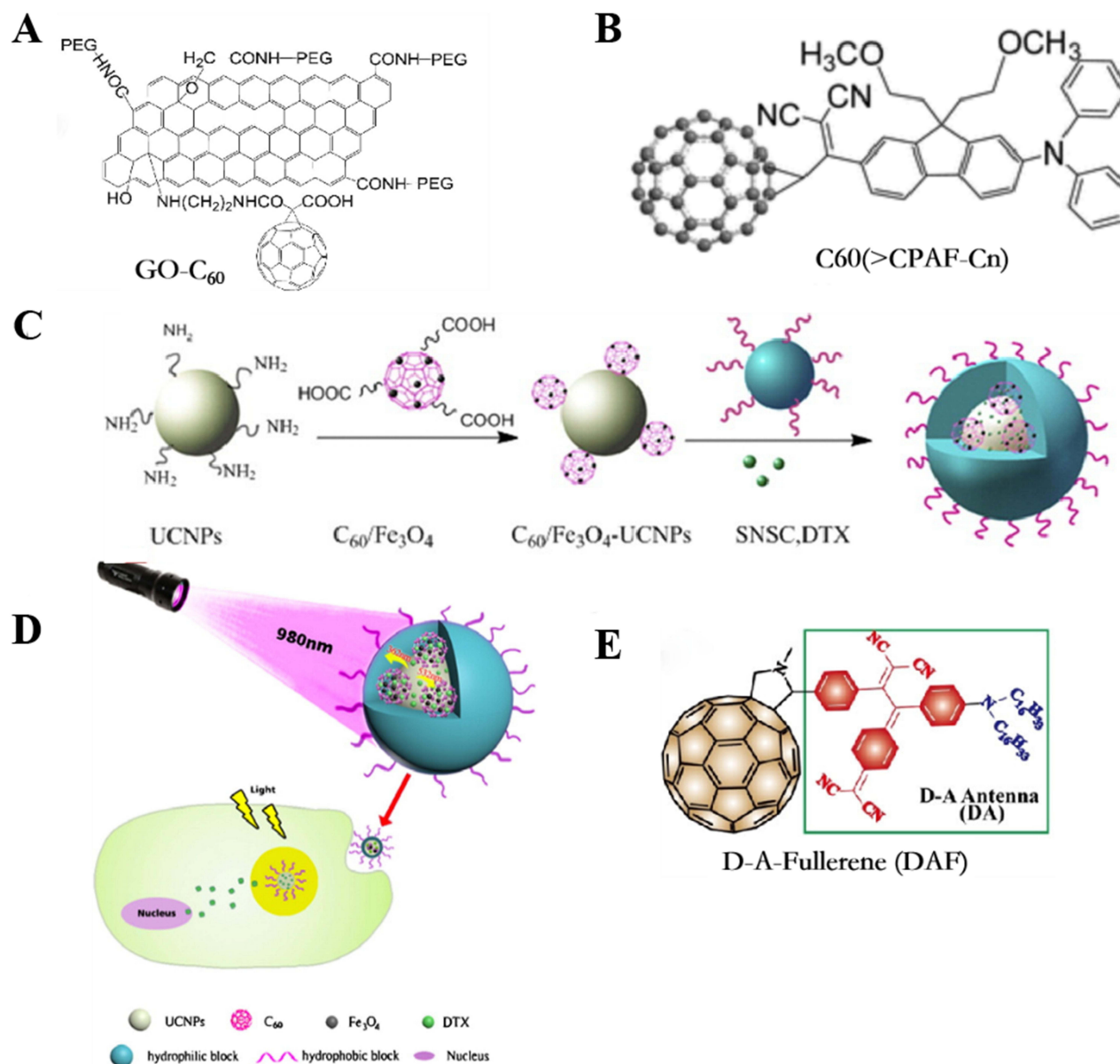


**Figure 4** Molecular structures and schematic illustration of the fullerenes modified with light-harvesting antennas. **(A)** Molecular structures of GO-C<sub>60</sub>. Adapted from *Biosens Bioelectron*, volume 89, Li Q, Hong L, Li HG, Liu CG. Graphene oxide-fullerene C<sub>60</sub> (GO-C<sub>60</sub>) hybrid for photodynamic and photothermal therapy triggered by near-infrared light. 477–482, Copyright 2017, with permission from Elsevier.<sup>16</sup> **(B)** Molecular structures of C<sub>60</sub>(>CPAF-Cn). Reprinted from Chiang LY, Padmawar PA, Rogers-Haley JE, et al. Synthesis and characterization of highly photoresponsive fullerene dyads with a close chromophore antenna-C<sub>60</sub> contact and effective photodynamic potential. *J Mater Chem*. 2010;20(25):5280–5293.<sup>90</sup> **(C)** Schematic illustration of the preparation of C<sub>60</sub>/Fe<sub>3</sub>O<sub>4</sub>-UCNPs@DTX@SNSC DAF NPs. Reprinted from *Nanomedicine*, volume 12(7), Du B, Han S, Zhao F, et al. A smart upconversion-based light-triggered polymer for synergistic chemo-photodynamic therapy and dual-modal MR/UCL imaging. 2071–2080, Copyright (2016), with permission from Elsevier.<sup>92</sup> **(D)** The anti-tumor mechanism of C<sub>60</sub>/Fe<sub>3</sub>O<sub>4</sub>-UCNPs@DTX@SNSC. Reprinted from.<sup>92</sup> **(E)** Molecular structures of DAF. Reprinted from Shi H, Gu R, Xu W, et al. Near-Infrared light-harvesting fullerene-based nanoparticles for promoted synergistic tumor phototheranostics. *ACS Appl Mater Interfaces*. 2019;11(48):44970–44977. Copyright (2019) American Chemical Society.<sup>93</sup>

mechanism of C<sub>60</sub>/Fe<sub>3</sub>O<sub>4</sub>-UCNPs@DTX@SNSC was shown in Figure 4D. In vitro and in vivo experiments demonstrated that the C<sub>60</sub>/Fe<sub>3</sub>O<sub>4</sub>-UCNPs@DTX@SNSC synergistically killed tumor cells by targeted release of DTX and massive generation of ROS under 980 nm light irradiation.<sup>92</sup> Shi et al covalently grafted a D-A antenna onto the surface of fullerenes, creating NIR light-harvesting fullerene-based nanoparticles (DAF NPs) (Figure 4E).<sup>93</sup> The addition of the D-A antenna shifted the absorption wavelength of fullerene from 532 (green region) nm to 720 nm (NIR region). Under 720 nm laser irradiation, the ROS generated by DAF NPs increased the degradation rate of DPBF (an ROS probe) from 20% (for pure fullerene) to 80%, indicating increased ROS production. Moreover, DAF NPs also generated substantial heat for photothermal therapy (PTT), demonstrating a synergistic photodynamic and photothermal effect in cancer therapy using a HeLa cell mouse model.<sup>93</sup>

It is worth noting that the position of light-harvesting antennas in relation to fullerenes also affects photodynamic performance to a certain extent. Antoku et al investigated the coexistence of light-harvesting antenna molecules, such as DiD (1,1-dioctadecyl-3,3,3,3-tetramethylindodicarbocyanine, dialkylated carbocyanine lipid membrane probes), and  $C_{60}$  in lipid bilayers using a biomimetic approach inspired by photosynthesis. The quantum yield of energy transfer between DiD and  $C_{60}$  was found to be less than 50% due to approximately 50% fluorescence quenching of DiD caused by  $C_{60}$  transfer within the lipid membranes.<sup>118</sup> Nevertheless, when the original  $C_{60}$  was replaced with  $C_{60}$  derivatives, moving  $C_{60}$  closer to the surface of the liposome, stronger photodynamic activities and increased ROS generation were observed compared to the original  $C_{60}$  located in the hydrophobic core. This could be attributed to the shorter distance between  $C_{60}$  and DiD or dissolved oxygen, making energy transfer from DiD to  $C_{60}$  more efficient. Therefore, when modifying the surface of fullerenes with fluorescent antennas, it is important to consider not only the energy transfer between different moieties but also the influence of their relative positions on the overall photodynamic performance.

Furthermore, to minimize damage to normal cells during PDT, it is crucial to design and develop PS that are responsive to the tumor microenvironment. Tang et al synthesized a pH-responsive PS  $C_{60}$ -RB by introducing a fullerene unit onto rhodamine B hydrazide. Under acidic conditions, the spiro-lactam structure of  $C_{60}$ -RB can be activated into its ring-open form,  $C_{60}$ -RB-H, which facilitates the transition to the excited triplet state. This transition enhances the visible light absorption of the fullerene component and the fluorescence of the RB-H moiety. The complex exhibits efficient intersystem crossing, reducing the energy gap between the singlet state and the triplet state to 0.017 eV, thus successfully creating pH-activable PS for the modulation of the triplet state. Experimental results demonstrate that at a pH of 5.0,  $C_{60}$ -RB displays enhanced fluorescence and efficient  $^1O_2$  generation, indicating excellent therapeutic potential in bioimaging and PDT for tumors.<sup>119</sup>

## Fullerenols

Biomedical application of fullerenes is severely restricted by their poor water solubility, which leads to ineffective dispersion in biological systems, poor targetability and high-dose cytotoxicity.<sup>120</sup> Functionalization of the fullerene surface with hydroxyl groups to generate polyhydroxyl fullerene derivatives is a promising strategy to overcome these drawbacks and fully exploit their anti-tumor potential. The resulting fullerene derivatives, fullerlenols ( $C_{60}(OH)_n$ ), possess significantly enhanced hydrophilicity with the anti-tumor properties of fullerenes well-preserved.<sup>121</sup>

Similar to fullerenes, fullerlenols are also capable of generating ROS under light irradiation. It is observed that water-soluble fullerlenols are more likely to induce cell apoptosis through the mitochondrial pathway rather than cell-membrane disruption.<sup>40</sup> The presence of multiple hydroxyl groups on the surface of fullerlenols brings about enhanced oxidation activities compared to fullerenes in a concentration-dependent manner.<sup>122</sup> Guo et al discovered that at high concentrations,  $C_{60}(OH)_n$  ( $n = 18-22$ ) exhibited an inhibitory effect on the human acute myeloid leukemia cell line K562, whereas at low concentrations, tumor cell growth promotion was observed. When the concentration of  $C_{60}(OH)_n$  ( $n = 18-22$ ) exceeded 160  $\mu M$ , K562 cells underwent morphological changes, and apoptotic bodies appeared. Further experiments revealed that the mitochondrial membrane potential of the cells decreased and the cell cycle was arrested at the G2 phase, ultimately leading to cell apoptosis. It was speculated that  $C_{60}(OH)_n$  ( $n = 18-22$ ) induced spontaneous apoptosis and cell death through oxidation by releasing ROS.<sup>94</sup>

In addition to be used in PDT, fullerlenols have shown potential to inhibit the metastasis of tumor cells. Tumor metastasis involves the transformation of tumor cells from a static state to a motile state, accompanied by the dynamic assembly and aggregation of actin. Qin et al demonstrated that fullerlenols not only induced cell death through PDT but also inhibited tumor cell metastasis by interfering with the physiological balance of G-actin and F-actin. Intravenous injection of small-sized fullerlenol nanoparticles ( $d = 2$  nm) reduced the formation of filopodia in MCF-7 and MDA-MB-231 breast cancer cells, altered the distribution of integrins in the cells, disrupted actin filaments and reduced cell activities. As a result, the ability of MCF-7 breast cells to pass through blood vessels was diminished, thereby inhibiting further metastasis of breast cancer cells to the lungs.<sup>51</sup> Jiao et al also reported that  $C_{60}(OH)_{20}$  exhibited *in vivo* anti-tumor and anti-metastasis activities in an EMT-6 breast cancer metastasis model. The inhibition of tumor growth and metastasis by fullerlenols *in vivo* may be attributed to their induction of oxidative stress in tumor tissue and inhibition of vascular endothelial growth factor formation, reducing tumor vascular density and impairing the nutritional supply to tumor cells.<sup>95</sup> Furthermore, in general, bone marrow mesenchymal

stem cells (BDMSCs) can be recruited to the tumor microenvironment, where they transform into malignant cells and further attract tumor cells to metastasize to the bone marrow, promoting bone metastasis.<sup>123</sup> Nie et al discovered that  $C_{60}(OH)_{22}$  can function as an inhibitor to weaken the cascade between BDMSCs and 4T1 breast cancer cells, inhibiting metastasis. By regulating the mitogen-activated protein kinase (MAPK) signaling pathway,  $C_{60}(OH)_{22}$  inhibited the activation of the NF- $\kappa$ B transcription factor which is often activated in malignant tumors. Consequently, phosphorylation of the p65 protein was suppressed and key paracrine factors involved in malignant progression (eg VEGF-A, IL-1 $\alpha$  and TGF- $\beta$ ) were down-regulated, reducing the metastasis of both BDMSCs and tumor cells, thereby inhibiting tumor metastasis to the bone.<sup>56</sup>

Being highly efficient antioxidants, fullerlenols can be used as protective agents in radiotherapy for cancer treatment.<sup>24</sup> ROS generated during radiotherapy inflict harm to normal tissue as well as to tumors, and fullerlenols, endowed with superior ROS-scavenging abilities, can protect normal tissue from radiation damage.<sup>124,125</sup> In vivo experiments have shown that at doses of 100–300 mg/kg i.p., fullerlenols exhibited a superior protective effect on the spleen, the small intestines and the lungs against X-ray radiation (8 MV) than the commonly used radioprotective drug amifostine (300 mg/kg i.p.).<sup>96</sup> Cai et al investigated the radioprotective effect of  $C_{60}(OH)_{24}$  under whole-body  $\gamma$ -irradiation. It was found that a 2-week pretreatment with  $C_{60}(OH)_{24}$  effectively protected the liver and the spleen from radiation-induced impairment of immune and mitochondrial functions and antioxidant defense deterioration, and reduced whole body irradiation-induced mortality without noticeable toxicity.<sup>97</sup>

Furthermore, fullerlenols can serve as potential protective agents in chemotherapy. The most widely used drugs in chemotherapy are anthracyclines (such as doxorubicin, (DOX)) with excellent anti-tumor effectiveness.<sup>126–128</sup> However, anthracyclines can cause systemic oxidative stress that leads to serious side effects.<sup>129</sup> Fullerlenols can counteract the harmful effects of anthracyclines by scavenging free radicals, alleviating the side effects of chemotherapy.<sup>98–100,127,130</sup> Chaudhuri et al connected fullerlenols and DOX through a carbamate linker and obtained a complex conjugate with ultra-high DOX drug loading rate.<sup>99</sup> The complex was relatively stable in PBS solution, but exhibited efficient DOX release when co-cultured with tumor cells. Compared with free DOX, the fullerlenol-DOX (Ful-DOX) conjugate was more effective in inhibiting the in vitro proliferation of multiple cancer cell lines (mouse melanoma cell line B16-F10, mouse lung cancer cell line LLC1 and metastatic human breast cancer cell line MDA-MB-231) (Figure 5A). In a mouse model, the Ful-DOX exhibited anti-tumor efficacy equivalent to free DOX but without the systemic toxicity of free DOX on the spleen and the heart (Figure 5B).<sup>99</sup> Jović et al constructed a nanocomposite material of fullerlenols and DOX (FNP/DOX). Compared to free DOX of the same concentration, the FNP/DOX significantly increased the uptake of DOX in MCF-7 and MDA-MB-231 cell lines and effectively reduced their viability through DNA damage. The FNP/DOX also effectively reduced the incidence of brain, cardiovascular and eye malformations through free radical clearance.<sup>100</sup> Injac et al investigated the potential hepatoprotective effect of  $C_{60}(OH)_{24}$  against DOX-induced liver toxicity in rats with breast cancer. Treatment with DOX in the absence of  $C_{60}(OH)_{24}$  resulted in a significant increase in the level of lactate dehydrogenase, as well as in levels of oxidative stress indicators (malondialdehyde, glutathione, glutathione peroxidase, total antioxidant status, glutathione reductase, catalase and superoxide dismutase), indicating the hepatic toxicity of DOX. However, when DOX and  $C_{60}(OH)_{24}$  were co-applied, levels of all indicators significantly decreased, suggesting that  $C_{60}(OH)_{24}$  mitigated the hepatotoxicity of DOX through ROS clearance.<sup>98</sup> Srdjenovic et al also demonstrated that adding  $C_{60}(OH)_{24}$  prevented DOX-induced oxidative stress in rat kidneys, testes and lungs.<sup>130</sup> These findings suggest that fullerlenols can be used as promising protective agents in chemotherapy.

Furthermore, fullerlenols can attack tumors by activating immune cells. During the immunogenic death of tumor cells, certain TAAs such as CRT are released, promoting the maturation of DCs. CRT is exposed on the surface of apoptotic tumor cells as a signal of “eat me” that activates the phagocytosis of the cells by DCs, while CD47 is exposed as a signal of “do not eat me”.<sup>131</sup> Chen et al found that fullerlenol nanoparticles (FNPs) induced stress responses of the endoplasmic reticulum, triggering CRT exposure on 7 types of tumor cells and effectively promoting programmed tumor cell clearance by phagocytes. Additionally, using the FNPs with anti-CD47 monoclonal antibody (mAb) was found to further enhance anti-tumor effectiveness. When used with half-dose anti-CD47 mAb, FNPs achieved similar effectiveness in treating subcutaneous glioblastoma U87MG and in situ osteosarcoma 143B to using full-dose anti-CD47 mAb alone, while promoting the M2-to-M1 repolarization of macrophages in the tumor microenvironment.<sup>88</sup>

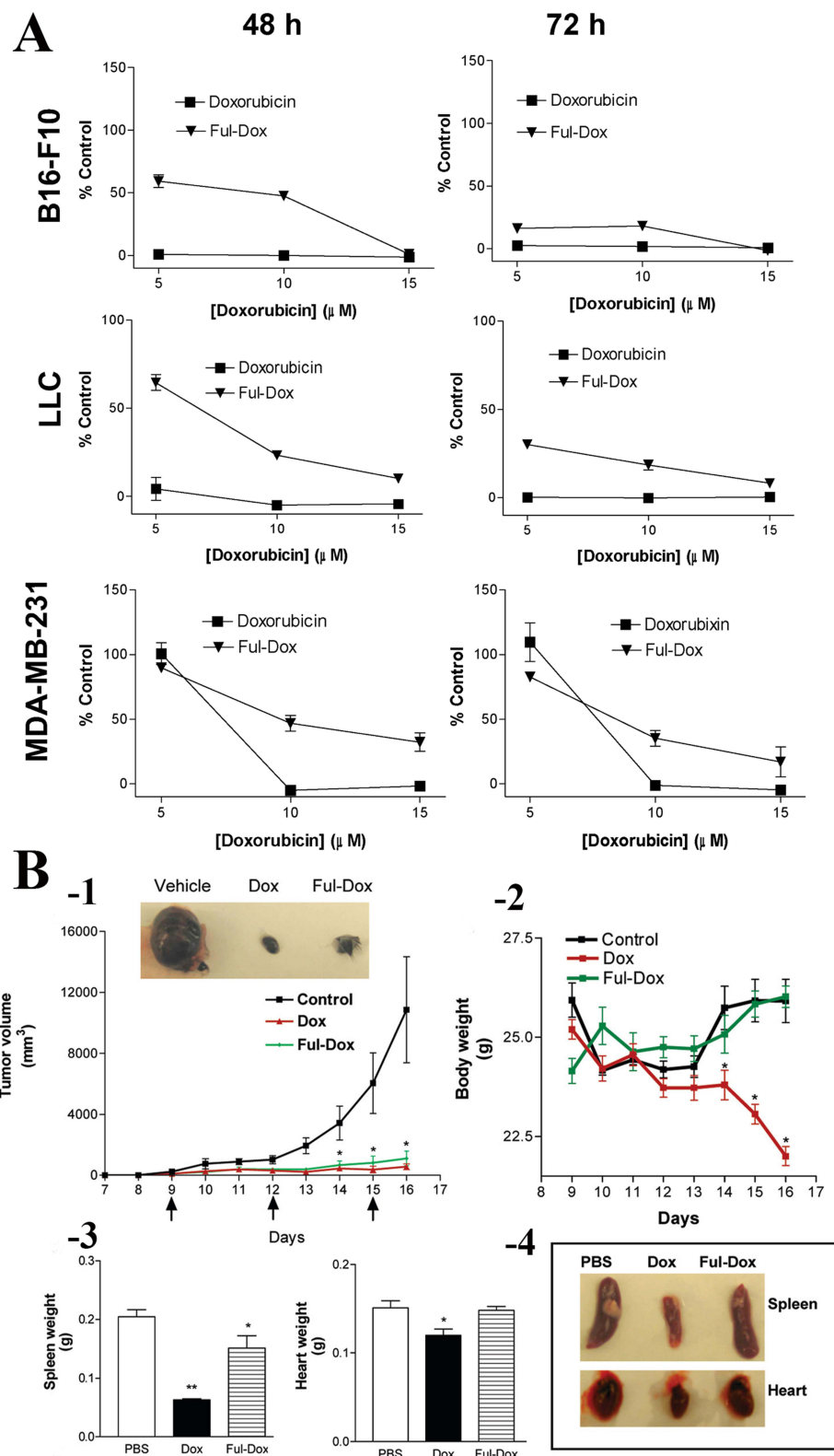


**Figure 5** Synthesis mechanism of the Ful-Dox conjugate and its anti-tumor effects. **(A)** Comparison of in vitro anti-tumor efficacy of Ful-Dox and free DOX alone. **(B)** In vivo efficacy of Ful-Dox conjugate nanoparticles in a mouse melanoma model. Line chart of tumor volume (-1), body weight (-2), spleen and heart weight (-3) after injection of Ful-DOX, DOX and PBS over time ( $P < 0.05$ ). Pictures of representative tumors from each treatment group are shown in (-4). All data shown are mean  $\pm$  SE of  $n = 4-5$  per treatment group and were subjected to statistical analysis (\* $P < 0.05$ ; \*\* $P < 0.001$  ANOVA followed by Newman Keul post hoc test). Reprinted from Chaudhuri P, Paraskar A, Soni S, Mashelkar RA, Sengupta S. Fullerene-cytotoxic conjugates for cancer chemotherapy. *ACS Nano*. 2009;3(9):2505-2514. Copyright (2009) American Chemical Society.<sup>99</sup>

## Metallofullerenes

Metallofullerenes, formed by encapsulating metal atoms or clusters inside the hollow structure of fullerenes, exhibit unique properties and have been explored for their therapeutic potential in tumor treatment.<sup>132</sup> These compounds not only retain the inherent properties of fullerenes but also modulate the tumor microenvironment, inhibiting tumor cell growth and metastasis.<sup>133</sup> Wang et al initially reported that  $\text{Gd}@C_{82}(\text{OH})_{22}$ , a metallofullerenol where  $\text{Gd}^{3+}$  ions are encapsulated within  $C_{82}$ , when administrated at low doses, exhibited similar anti-tumor effectiveness as conventional chemotherapy drugs without cytotoxicity to normal tissue.<sup>101,134,135</sup> Further studies demonstrated that  $\text{Gd}@C_{82}(\text{OH})_{22}$  can attack tumors by various mechanisms including inhibition of tumor angiogenesis, regulation of cellular immunity and inhibition of tumor metastasis.<sup>77,101,134,136</sup>

One potential mechanism by which metallofullerenes inhibit tumor metastasis is confining tumors through the formation of collagen “cages”. Meng et al reported that  $\text{Gd}@C_{82}(\text{OH})_{22}$  effectively reduced MMP production and activities while stabilizing collagen, impeding the MMP-induced degradation of ECM and stimulating the formation of collagen microfibers around human breast cancer cells (Figure 6A).<sup>101</sup> Consequently, the tumor was engaged in a dense fibrous structure that hindered its growth and subsequent metastasis. The thickness of the fibrous enclosure in the presence of  $\text{Gd}@C_{82}(\text{OH})_{22}$  increased to more than five-fold that of the control group, attesting to the efficacy of  $\text{Gd}@C_{82}(\text{OH})_{22}$  in building collagen cages to restrain tumor progression and metastasis (Figure 6B). Another noteworthy advantage of employing metallofullerenes in this context is their non-cytotoxic nature towards normal cells, rendering them a safer modality of tumor treatment. Kang et al further analyzed the interaction of  $\text{Gd}@C_{82}(\text{OH})_{22}$  with MMP through molecular-dynamics simulation, and found that  $\text{Gd}@C_{82}(\text{OH})_{22}$  impaired MMP-9 functions in an exosite way by allosteric regulation.<sup>102</sup>  $\text{Gd}@C_{82}(\text{OH})_{22}$  nanoparticles first cluster and form trimers stepwise, and eventually bind to MMP-9 molecules through electrostatic and hydrophobic interactions (Figure 6C), and  $\text{Gd}@C_{82}(\text{OH})_{22}$  indirectly inhibits MMP-9 activity by binding at the ligand specificity S1' loop.<sup>102</sup> However, the hydrophobicity of the aromatic carbon cage structure can somewhat weaken its binding affinity with the S1' loop. To enhance binding affinity, Chen et al introduced charged functional groups of varying sizes on the surface of metallofullerol, targeting the charged residues near the S1' loop. This modification enhanced electrostatic interactions, thereby improving binding stability. Moreover, the higher the net charge of the functional groups, the stronger the binding affinity.<sup>137</sup> Furthermore,  $\text{Gd}@C_{82}(\text{OH})_{22}$  can exhibit a bridging effect among collagen molecules, greatly restricting their relative rotation and crosslinking them to stabilize the collagen triplex structure to prevent MMP-induced degradation.<sup>103</sup> Liu et al further analyzed the molecular mechanism by which  $\text{Gd}@C_{82}(\text{OH})_{22}$  promotes Collagen Type I & III formation. It was found that  $\text{Gd}@C_{82}(\text{OH})_{22}$  can promote the binding between TNF- $\alpha$  and tumor necrosis factor receptors 2 (TNFR2), while simultaneously inhibiting the interaction between TNF- $\alpha$  and TNFR1, thus activating the TNFR2/p38 MAPK signaling pathway to increase cellular collagen expression in fibrosarcoma cells and human primary lung cancer-associated fibroblasts.<sup>55</sup> Pan et al further discovered that  $\text{Gd}@C_{82}(\text{OH})_{22}$  can suppress pancreatic cancer cell metastasis by down-regulating the expression of metastasis-related protein 1, histone deacetylase 1, hypoxia-inducible factor-1R and MMP-2/9, while up-regulating the expression of reversion-cysteine proteins,<sup>104</sup> suggesting that  $\text{Gd}@C_{82}(\text{OH})_{22}$  may serve as a potential inhibitor to suppress pancreatic cancer cell invasion and metastasis.

Disruption of the tumor vasculature is a promising strategy for inhibiting tumor growth, as it can induce tumor cell starvation. Guan et al proposed a tumor vasculature-oriented PDT (V-PDT) (Figure 7A) utilizing photodynamically produced ROS to kill vascular endothelial cells in the oxygen-rich environment of the tumor vasculature, cutting off tumors from nutrient supply.<sup>71</sup> By adding  $\beta$ -alanine to an alkali aqueous solution containing  $\text{Gd}@C_{82}$ , a metallofullerene Gd-Ala (Figure 7B) was produced. Compared with traditional tumor cell-oriented PDT (C-PDT), V-PDT requires a significantly reduced time interval between PS injection and light irradiation, killing 4T1 tumor cells and tumor vascular endothelial cells simultaneously by mass production of ROS. A tumor vascular DSFC model implanted with 4T1-luc tumor cells was established to monitor the tumor vascular morphology in real-time. Hemorrhage was observed at the periphery of the tumor vasculature 20 min after the start of V-PDT and continued for another 40 min. Segments of tumor vessels then began to collapse with severe hemorrhage, as indicated by the red circles in Figure 7C. Destruction of vascular endothelial-cadherin (VE-cadherin, responsible for intercellular connection) was also observed, causing the loss of intercellular

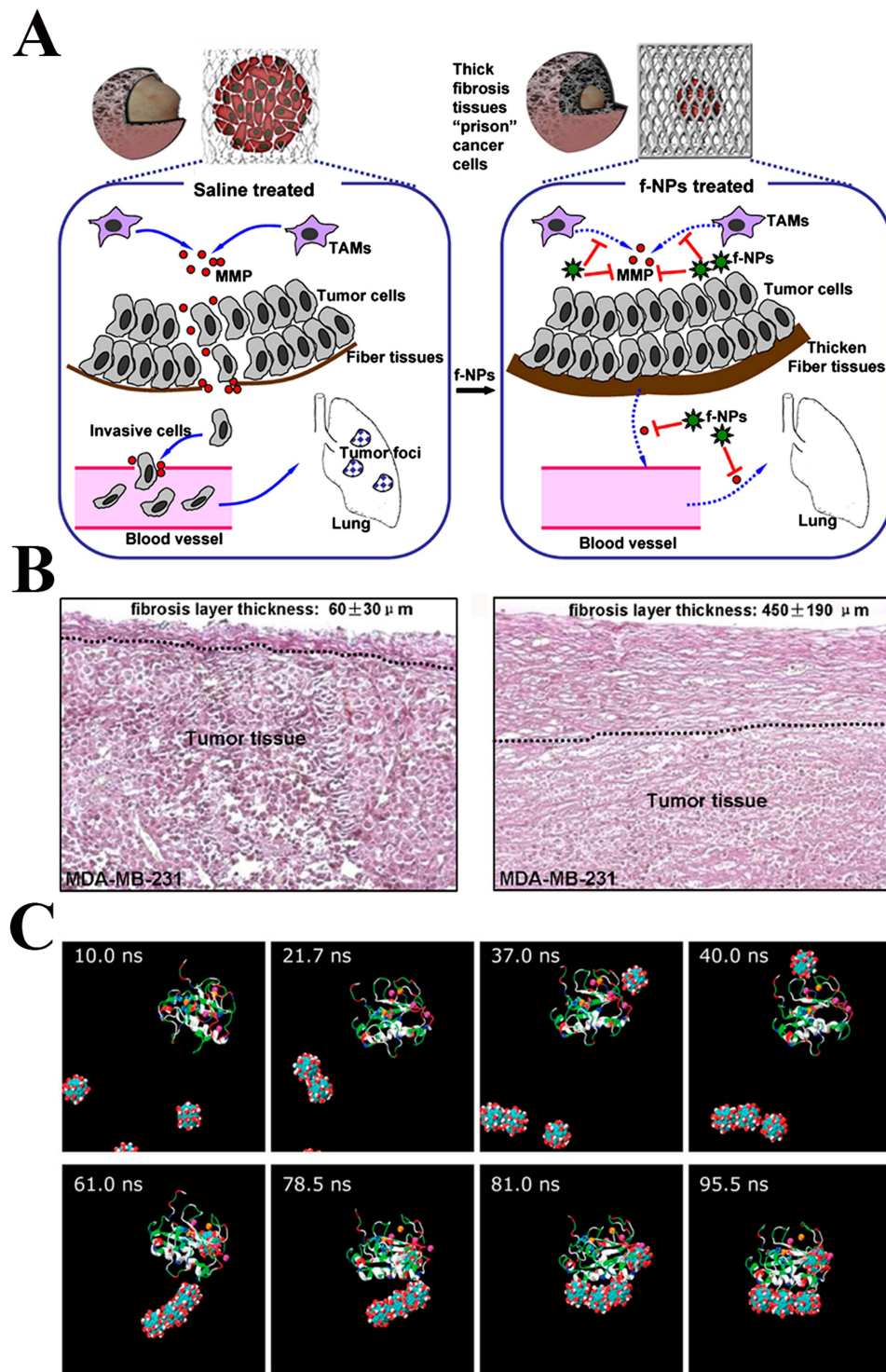


**Figure 6** Tumor encaging by  $\text{Gd}@C_{82}(\text{OH})_{22}$  therapy. The  $\text{Gd}@C_{82}(\text{OH})_{22}$  inhibits tumor metastasis by reducing MMP production and activity, stabilizing collagen and impeding ECM degradation, thereby forming a dense fibrous cage that engages the tumor to inhibit tumor metastasis. **(A)** Schematic presentation of tumor encaging by  $\text{Gd}@C_{82}(\text{OH})_{22}$ . Reprinted from *Nanomedicine*, volume 8(2), Meng H, Xing G, Blanco E, et al Gadolinium metallofullerenol nanoparticles inhibit cancer metastasis through matrix metalloproteinase inhibition: imprisoning instead of poisoning cancer cells. 136–146, Copyright 2012, with permission from Elsevier.<sup>101</sup> **(B)** Histological images of tumor tissue excised from the saline control group (left) and  $\text{Gd}@C_{82}(\text{OH})_{22}$ -treated group (right) of MDA-MB-231 xenograft mice. Reprinted from *Nanomedicine*, volume 8 (2), Meng H, Xing G, Blanco E, et al Gadolinium metallofullerenol nanoparticles inhibit cancer metastasis through matrix metalloproteinase inhibition: imprisoning instead of poisoning cancer cells. 136–146, Copyright 2012, with permission from Elsevier.<sup>101</sup> **(C)** Molecular dynamics of  $\text{Gd}@C_{82}(\text{OH})_{22}$  interacting with MMP-9. Reprinted from Kang SG, Zhou G, Yang P, et al, Molecular mechanism of pancreatic tumor metastasis inhibition by  $\text{Gd}@C_{82}(\text{OH})_{22}$  and its implication for de novo design of nanomedicine. *Proc Natl Acad Sci USA*. 2012;109:15431–15436. Copyright (2012) American Chemical Society.<sup>102</sup>

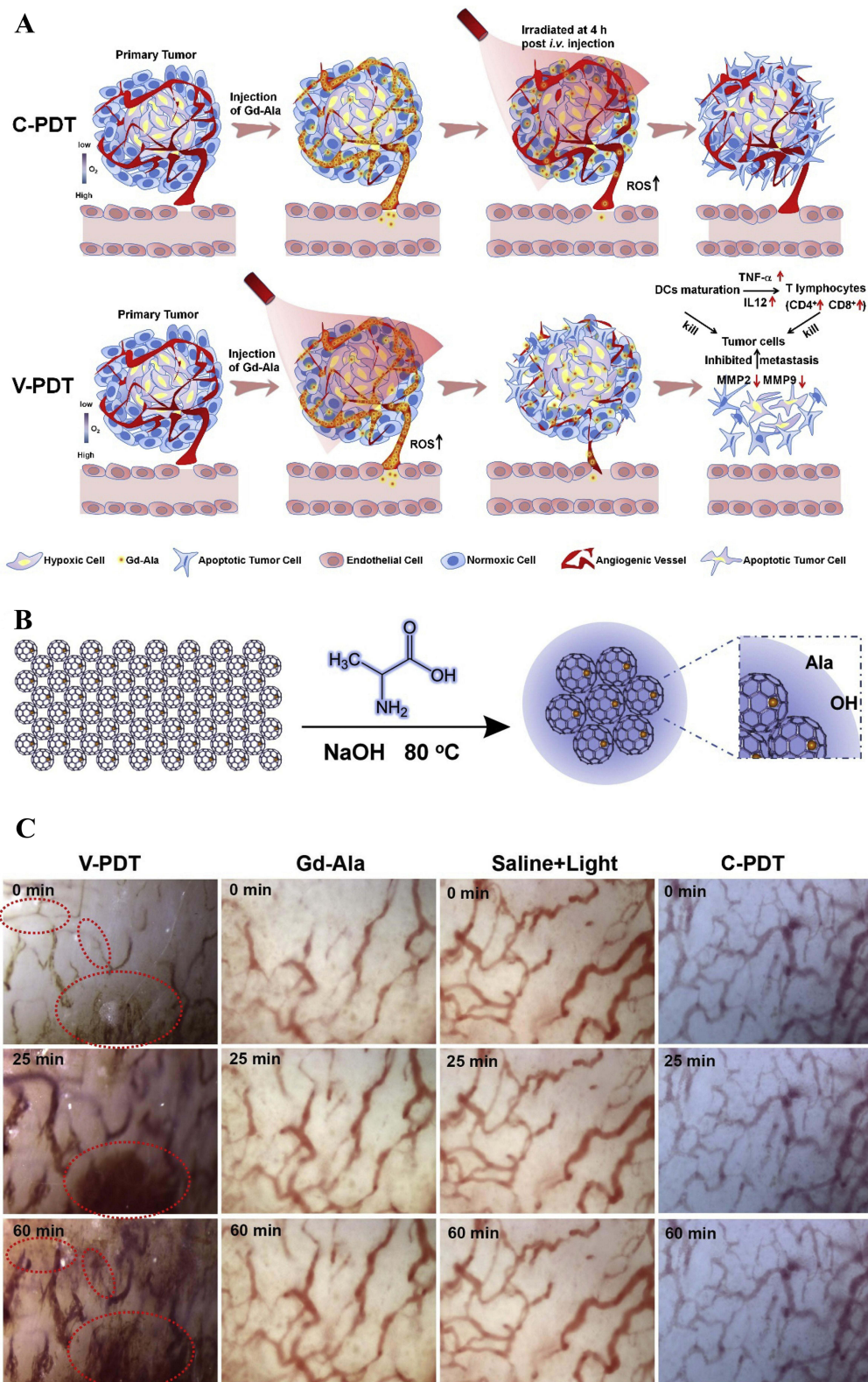


**Figure 7** Mechanism, synthesis route, and anti-tumor effects of Gd-Ala via C-PDT. **(A)** Schematic representation of C-PDT and V-PDT based on Gd-Ala. Compared to traditional C-PDT, V-PDT offers a shorter time between PS injection and light irradiation, simultaneously targeting 4T1 tumor cells and vascular endothelial cells through massive ROS production. **(B)** Schematic diagram of Gd-Ala preparation. **(C)** The real-time observation of the tumor vasculature under different treatments. Hemorrhage at the periphery of the tumor vasculature was observed 20 minutes after V-PDT initiation and continued for 40 minutes. Collapsed tumor vessels with severe hemorrhage are marked with red circles. Reprinted from *Biomaterials*, Volume 213, Guan M, Zhou Y, Liu S, et al. Photo-triggered gadofullerene: enhanced cancer therapy by combining tumor vascular disruption and stimulation of anti-tumor immune responses. 119218, Copyright 2019, with permission from Elsevier.<sup>71</sup>



connection between tumor vascular endothelial cells. In addition, Gd-Ala promoted the secretion of TNF- $\alpha$  and IL-12 by DCs, activating T lymphocytes and down-regulating the expression of MMP-2 and MMP-9 to inhibit tumor metastasis.<sup>71</sup> Lu et al synthesized  $\beta$ -alanine modified gadolinium-metallofullerene nanoparticles (GFNPs) that produced abundant  $^1\text{O}_2$  under irradiation, inducing rapid tumor necrosis by destroying VE-cadherin and reducing the secretion of CD31 by tumor vascular endothelial cells. The anti-tumor effectiveness of the GFNPs was found to be correlated to particle size, as smaller GFNPs exhibited the highest efficiency.<sup>106</sup>

Apart from photodynamic destruction of the tumor vasculature, metallofullerenes can also destroy tumor blood vessels by size expansion during phase change. Wang et al devised a novel anti-tumor strategy that specifically targets and eradicates poorly structured tumor blood vessels by intravenously injecting gadofullerene nanocrystals (GFNCs) that could enter the gaps between endothelial cells.<sup>18</sup> Under 200 Hz RF irradiation, the GFNCs underwent a phase change, resulting in acute size expansion and destruction of the tumor blood vessel endothelium, eventually leading to tumor necrosis and detachment (Figure 8A).<sup>18</sup> Moreover, Li et al observed a significant reduction in VE-cadherin expression in tumor blood vessels following treatment with GFNCs. The loss of intercellular connection between endothelial cells led to vascular leakage and collapse, thereby inducing hemorrhagic necrosis (Figure 8B).<sup>138</sup>

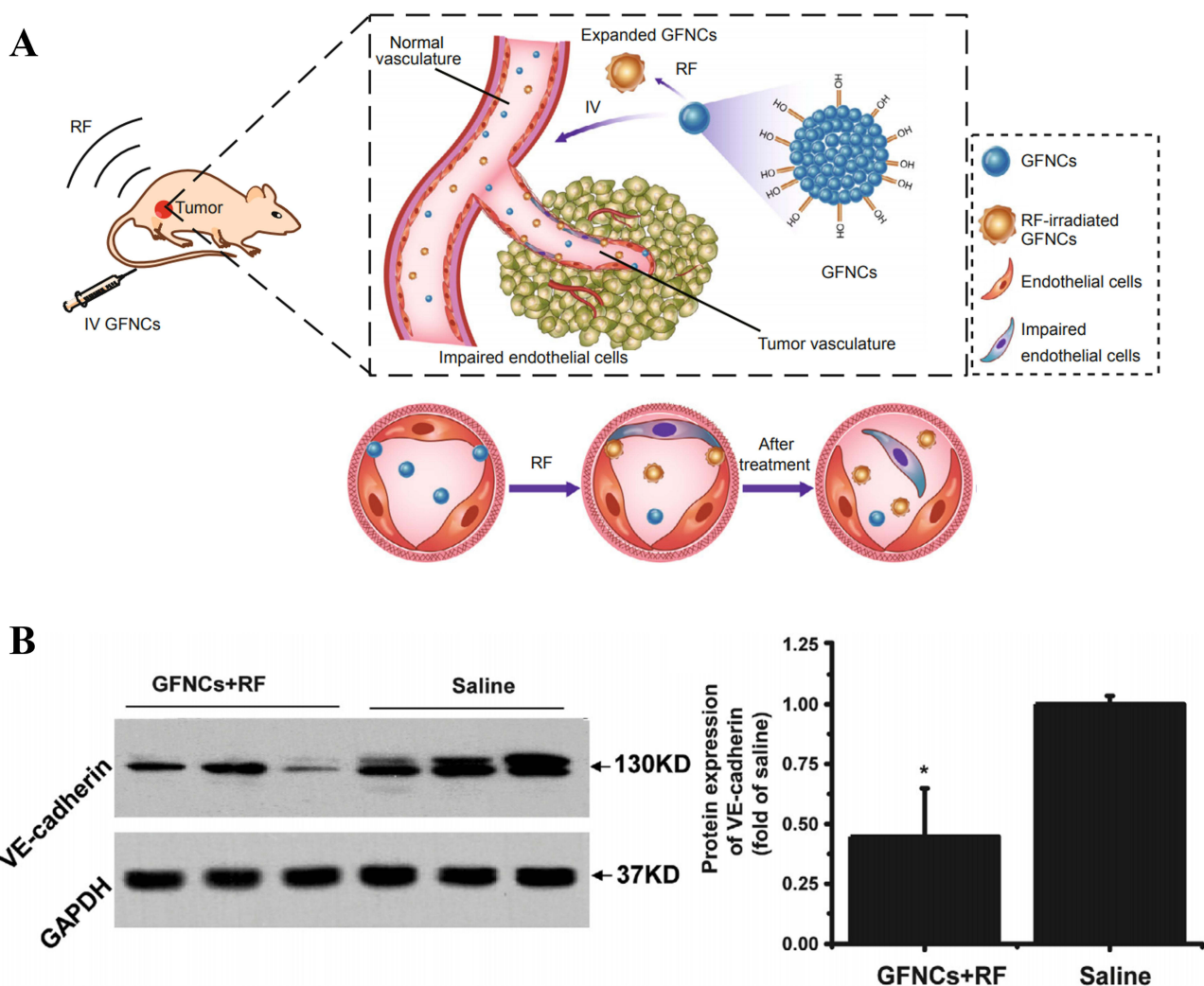


**Figure 8** Mechanism of RF-assisted GFNCs treatments and their impact on VE-cadherin expression. **(A)** Schematic draw of the anti-tumor mechanism of RF-assisted GFNCs treatments. The GFNCs accumulate in the lining of the tumor blood vessels due to EPR effect, and then undergo rapid size expansion and rotation under RF irradiation, inducing the exfoliation of endothelial cells. Reprinted from Zhen MM, Shu CY, Li J, et al. A highly efficient and tumor vascular-targeting therapeutic technique with size-expansive gadofullerene nanocrystals. *Sci China*. 2015;58(10):799–810, Springer Nature.<sup>18</sup> **(B)** The decrease of VE-cadherin expression in the tumors after a 6-h treatment by GFNCs + RF. \* $P < 0.05$  compared to the saline group. Adapted from *Biomaterials*. Volume 163, Li X, Zhen M, Deng R, et al. RF-assisted gadofullerene nanoparticles induces rapid tumor vascular disruption by down-expression of tumor vascular endothelial cadherin. 142–153, Copyright 2018, with permission from Elsevier.<sup>138</sup>

Recent studies have shed light on the immunostimulatory properties of metallofullerenes, demonstrating their potential to activate the immune system.<sup>76–78</sup> Metallofullerenes can promote the maturation of DCs, regulate the differentiation of T cells and TAMs, and facilitate the phagocytosis of tumor cells by the immune system. The maturation process of DCs involves various molecular regulations, including internalization of TAAs, upregulation of co-stimulatory molecules such as CD80, CD86 and CD40, and secretion of a range of cytokines including IL-2, IL-5, IL-8 and IL-12.<sup>139,140</sup> Yang et al reported that [Gd@C<sub>82</sub>(OH)<sub>22</sub>]<sub>n</sub> nanoparticles upregulated relevant cytokines and increased the expression of maturation markers (eg CD83, CD80, CD86 and human leukocyte antigen-ABCDR) in a dose-dependent manner, indicating their potential to promote DC maturation. Additionally, the [Gd@C<sub>82</sub>(OH)<sub>22</sub>]<sub>n</sub> nanoparticles were found to enhance T cell activation toward the Th1 phenotype, implying their capacity to stimulate cell-mediated immune responses.<sup>84</sup> Guan et al observed similar results with Gd-Ala, whose activation by irradiation upregulated the expression of CD86 and CD80, promoting DC maturation.<sup>71</sup> Besides, Gd-Ala also promoted the secretion of TNF- $\alpha$  and IL-12, activating the cytotoxic activity of CD8<sup>+</sup> T lymphocytes, which induced anti-tumor immunity.

Metallofullerenes have also been reported to induce the phenotype transition of TAMs. Li et al found that  $\beta$ -alanine-modified Gd@C<sub>82</sub> (GF-Ala) nanoparticles (Figure 9A) were efficiently internalized by TAMs and induced an M2 to M1 phenotype transition (Figure 9B-1). Infiltration of cytotoxic T lymphocytes (CTLs) into tumor tissue was also increased (Figure 9B-2), triggering effective anti-tumor immunity and inhibition of tumor growth (Figure 9C). Additionally, using GF-Ala nanoparticles with a common anti-tumor drug anti-PD-L1 immune checkpoint inhibitor has been reported to achieve a superior synergistic treatment effect.<sup>89</sup> GF-Ala nanoparticles have also been found to bind to complement C1q, a key component of the complement system, leading to enhanced activation of the complement cascade that contributed to the elimination of lung cancer cells and boosting of anti-tumor immune response.<sup>105</sup>

Moreover, the nuclear magnetic effect of metal particles of gadolinium-metallofullerenes enables their use as contrast agents in magnetic resonance imaging (MRI). Wang et al developed a pH-responsive gadolinium-metallofullerene nanoparticle (GMF) by conjugating a pH-responsive polymer PEG-PDPA-DEA-NHS to amino-functionalized GMF (Gd<sub>3</sub>N@C<sub>80</sub>-NH<sub>2</sub>).<sup>141</sup> In this system, the nanoparticles serve as signal amplifiers for tumor detection and as drug release detection agents. Under normal physiological pH conditions, the metallofullerene and drugs are encapsulated within the hydrophobic core, resulting in weak MRI signals and slow drug release. However, in the acidic tumor microenvironment, the pH-responsive polymer undergoes a hydrophobic-to-hydrophilic transition, leading to amplified MRI signals and rapid drug release. This pH-responsive behavior allows targeted release of anti-tumor drugs in the tumor microenvironment.

## Fullerene-Biomacromolecule Derivatives

Fullerenes have also been extensively modified with biomacromolecules including amino acids, peptides and glucose to enhance their water solubility, biocompatibility, photodynamic properties and targeting capabilities.<sup>142–144</sup>

### Fullerenes Modified with Amino Acids

Fullerenes can be modified with amino acids such as glycine, L-proline, L-arginine, D-arginine, valine and phenylalanine through Prato reactions. Li et al chemically linked phenylalanine and glycine with C<sub>60</sub> to prepare two types of fullerene-amino acid nanoparticles (C<sub>60</sub>-phe and C<sub>60</sub>-gly).<sup>107</sup> These derivatives not only possess increased water solubility, but are also capable of generating abundant ROS through type II mechanism, exhibiting strong photodynamic activities in vitro. When human liver cancer cells SMMC-7721 were co-cultured with C<sub>60</sub>-phe and C<sub>60</sub>-gly under white light irradiation, cell division was significantly inhibited after 48 hours, and a substantial amount of ROS was produced through the photodynamic process, leading to DNA cleavage and cell apoptosis. No significant cytotoxicity was observed in the dark. Nalepa et al also observed that the C<sub>60</sub>-glycine-gemcitabine nanoconjugate (nano-C<sub>60</sub>GEM, Figure 10A) produced a large amount of ROS under blue LED irradiation, causing pancreatic cancer cell PAN02 to arrest in the S phase and ultimately inducing cell apoptosis.<sup>145</sup> Belik et al further compared the superoxide and <sup>1</sup>O<sub>2</sub> generation efficiency by three fullerene-amino acid derivatives (Val-C<sub>60</sub>, Ala-C<sub>60</sub> and Pro-C<sub>60</sub> (Figure 10B)) in an aqueous solution, and found that the photodynamic mechanism shifted from type II (<sup>1</sup>O<sub>2</sub> generation) to type I (superoxide generation). These derivatives

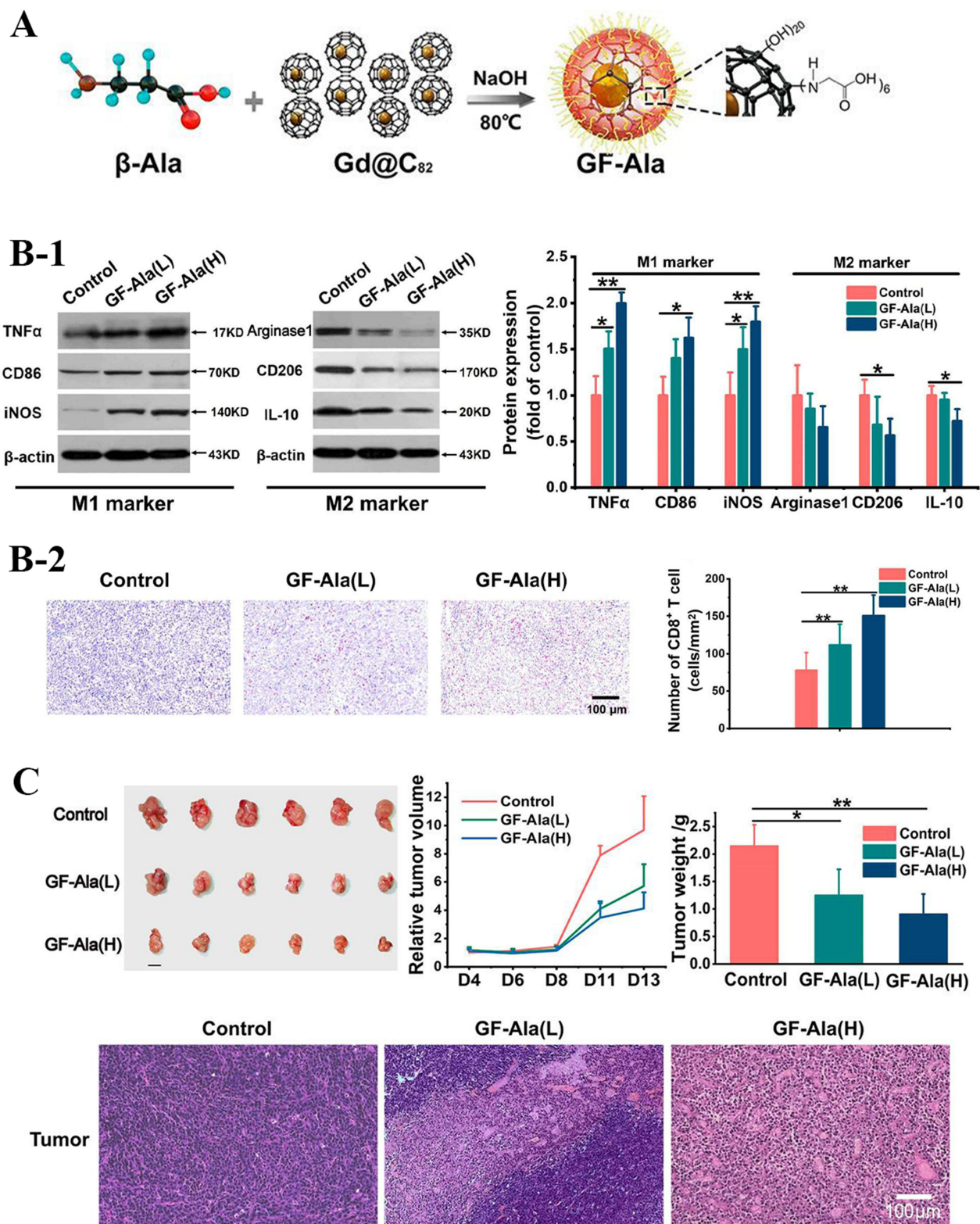


**Figure 9** Synthesis route of GF-Ala and its anti-tumor effects through immune system activation. Reprinted from Li L, Zhen MM, Wang HY, et al. Functional Gadofullerene nanoparticles trigger robust cancer immunotherapy based on rebuilding an immunosuppressive tumor microenvironment. *Nano Lett.* 2020;20(6):4487–4496. Copyright 2020, American Chemical Society.<sup>89</sup> (A) Schematic diagram illustrating the preparation of GF-Ala. (B) GF-Ala rebuilt immunosuppressive tumor environment (ITM) by polarizing TAMs to M1-type and increasing the infiltration of CTLs in tumor tissue. (B-1) Expression of M1 markers (TNF- $\alpha$ , CD86, iNOS) and M2 markers (IL-10, Arginase1, CD206) in tumor tissue audited via WB. (B-2) The immunofluorescence staining images and quantitative analysis for CD8. \* $p < 0.05$ ; \*\* $p < 0.01$ . (C) Anticancer effect of GF-Ala in BALB/c mice bearing subcutaneously inoculated 4T1 mouse breast tumors in vivo. Tumor growth profiles and weight of tumor-bearing mice during the observation and images of H&E stained slice of tumors after various treatments.

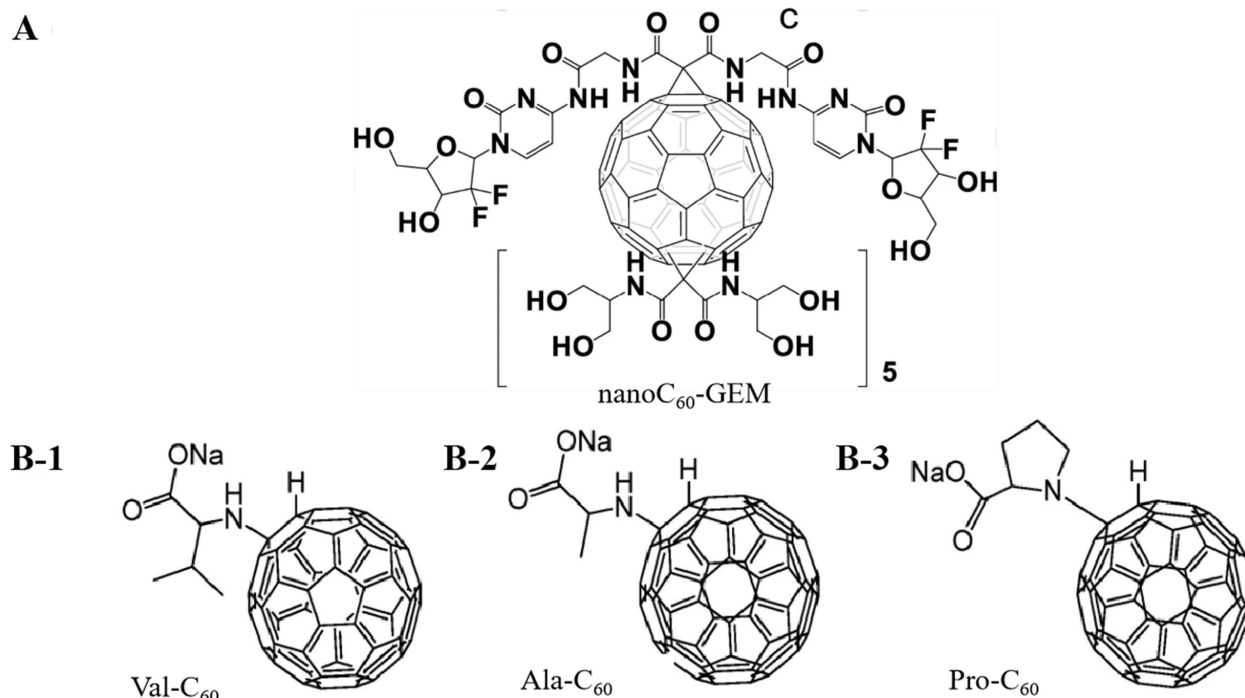


**Figure 10** Molecular structures of **(A)** nanoC<sub>60</sub>-GEM. Adapted from these studies. Creative Commons.<sup>144,146</sup> and **(B-1)**: Val-C<sub>60</sub>, **(B-2)**: Ala-C<sub>60</sub>, **(B-3)** Pro-C<sub>60</sub>. Reprinted from *Mol Biomol Spectrosc.* Volume 260. Belik AY, Rybkin AY, Goryachev NS, et al. Nanoparticles of water-soluble dyads based on amino acid fullerene C(60) derivatives and pyropheophorbide: synthesis, photophysical properties, and photodynamic activity, *Spectrochimica Acta Part A.* 260:119885, Copyright 2021, with permission from Elsevier.<sup>108</sup>

exhibited pronounced phototoxicity on HeLa cells, with IC<sub>50</sub> values of 9.2 mM, 9.2 mM and 12.2 mM, respectively, demonstrating their potential in PDT in hypoxic environments.<sup>108</sup>

Furthermore, leveraging the lipophilicity of fullerenes can improve the pharmacokinetics of low-lipophilicity drugs. Aminolevulinic acid (ALA) is a precursor of protoporphyrin IX, a PS that accumulates in tumor cells and generates ROS upon light activation, and is widely used clinically for the treatment of skin cancer and brain tumors. However, its low lipophilicity limits its ability to cross cell membranes and the blood-brain barrier, affecting the efficacy of PDT. To address this issue, Serda et al conjugated ALA with C<sub>60</sub> to synthesize C<sub>60</sub>-ALA nanoparticles, aiming to enhance the lipophilicity of ALA. Experimental results demonstrated that C<sub>60</sub>-ALA delivered a highly effective form of protoporphyrin IX in three cancer cell lines: MCF-7, HTC 116 and A549, thereby enhancing the intracellular accumulation of ALA and boosting its anti-tumor efficacy.<sup>146</sup> Li et al further modified the surface of C<sub>70</sub> with cyclodextrin and a peptide chain cRGDFk, resulting in the self-assembly of microspheres and the encapsulation of a hypoxia-activated prodrug tirapazamine, creating a hypoxia-sensitive PS system. Upon light irradiation, C<sub>70</sub> consumes O<sub>2</sub> to produce ROS to kill tumor cells. This in turn exacerbates the hypoxic state of the tumor microenvironment, activating tirapazamine to generate toxic free radicals that further attack tumors. This approach enables the synergistic treatment of deep-seated tumors in hypoxic conditions through a combination of PDT and hypoxia-activated chemotherapy.<sup>147</sup> Although numerous studies have demonstrated the cytotoxicity of fullerene-amino acid derivatives to tumor cells through photodynamic processes, there are significant differences in the photodynamic mechanisms and effects among different derivatives. These differences may be attributed to factors such as the modification site of the amino acid and the molecular size, necessitating further exploration and development.

In addition, certain fullerene-amino acid derivatives can bind to the Bruton's tyrosine kinase (BTK) protein, specifically inhibiting its activity and thereby suppressing tumor growth. BTK is overexpressed or abnormally activated in B cell-related hematologic malignancies, making it a crucial target in cancer therapy, particularly for B-cell lymphomas and chronic lymphocytic leukemia. Malarz et al modified fullerenes using diglycine malonate via Bingel-Hirsch cyclopropanation to produce a hexakis diglycinemethanofullerene nanomaterial. This nanomaterial can block the

formation of the BTK protein, thereby inhibiting its downstream molecular pathway and exhibiting significant anticancer properties against RAJI leukemia cells.<sup>148</sup>

Other biological macromolecules such as proteins can enhance the dispersion of fullerenes in physiological environments and prevent aggregation. Lysozyme has been shown to bind to C<sub>60</sub> and disperse them in water, forming a C<sub>60</sub>@lysozyme complex that retains the photoactivity of C<sub>60</sub>. This complex generated significant amounts of ROS under visible light irradiation while maintaining biocompatibility in the dark.<sup>149</sup> Giosia et al further utilized C<sub>70</sub>, which has a broader light absorption spectrum than C<sub>60</sub>, to prepare C<sub>70</sub>@lysozyme complexes that exhibited excellent optical and photoacoustic contrast for tracking their cellular uptake and intracellular localization. The complexes produced substantial amounts of ROS intracellularly under white light irradiation, effectively leading to tumor cell death.<sup>150</sup>

### Fullerenes Modified with Glucose

Sweet-C<sub>60</sub> is a family of glucose-functionalized fullerene nanomaterials with a strong affinity with glucose receptors, thereby facilitating its uptake by tumor cells.<sup>151–153</sup> Sweet-C<sub>60</sub> have garnered considerable attention due to their cancer-targeting capabilities as glucose baits for highly glucose-dependent tumors, particularly pancreatic ductal adenocarcinoma (PDAC).<sup>109</sup> Korzuch et al observed that sweet-C<sub>60</sub> modestly elevated glycolysis levels of pancreatic cancer cells at higher concentrations, indicating the cellular uptake of sweet-C<sub>60</sub> by the cancer cells.<sup>110</sup> Similarly, Barańska et al reported that treatment with sweet-C<sub>60</sub> resulted in increased expression of glucose transporter in pancreatic cancer cells due to enhanced glucose demand.<sup>109</sup> These findings may establish sweet-C<sub>60</sub> as a promising candidate for targeted drug delivery in pancreatic cancer therapy. Notably, hexakis-glucosamine C<sub>60</sub> derivatives have been found to accumulate within the nucleus of pancreatic stellate cells, a crucial subcomponent of PDAC, and demonstrate potent photodynamic cytotoxicity upon irradiation with blue and green light.<sup>111</sup> Moreover, Glycofullerenes have been reported to impede the growth and metastasis of human pancreatic cancer by down-regulating the expression of non-receptor tyrosine kinases Fyn A and BTK, which are crucial for cell signaling pathways that promote tumor cell migration and invasion. By inhibiting these kinases, glycofullerenes effectively disrupt these signaling pathways, leading to reduced tumor cell motility and metastasis.<sup>154</sup> Additionally, glycofullerenes can modulate the polarity of TAMs and regulate tumor immunity. Wang et al reported that dicarboxy fullerenes modified with mannose acted as an immunomodulator to selectively polarize TAMs and significantly enhance anti-tumor immunity. Experimental results demonstrated that the mannose-modified fullerenes were abundantly taken up by immunosuppressive M2 macrophages, effectively repolarizing them into anti-tumor M1 macrophages.<sup>155</sup>

## Conclusions and Perspectives

This review provides a comprehensive summary and discussion on the anti-tumor mechanisms and application of fullerenes and their derivatives in anti-tumor therapy. Firstly, the anti-tumor mechanisms of fullerenes are introduced in detail. The photodynamic properties of fullerenes endow them with the ability to generate a significant amount of free radicals under light irradiation, leading to the destruction of tumor cells and vasculature. Additionally, fullerene derivatives can disrupt the cytoskeleton of tumor cells to reduce their migration capabilities, or inhibit MMP secretion and activities to form dense fibrous structures to enwrap the tumor tissue, inhibiting tumor metastasis. When combined with metal ions or clusters, fullerenes can destroy the tumor vasculature by undergoing acute size expansion during phase transition under RF radiation. Fullerene derivatives can also activate the body's immune responses to eliminate tumor cells. Furthermore, the antioxidant properties of fullerenes enable them to scavenge free radicals, providing protection for normal tissue in conventional chemotherapy or radiotherapy.

To achieve the above-mentioned functions, surface modification of fullerenes is usually required. Grafting light-harvesting antennas on the fullerene surface can effectively shift the absorption range of fullerenes to the NIR region, increasing their ability to treat deep-seated tumors. Surface modification of fullerenes into fullereneols and metallofullerenes not only significantly improves water solubility but also endows them with functions such as tumor vasculature disruption, tumor metastasis inhibition and antitumor immune response activation. Furthermore, modification with biomacromolecules such as sugar moieties enhances the targeting and delivery efficiency of fullerenes in treating highly glucose-dependent tumors. Currently, extensive research is ongoing to construct new fullerene derivatives to obtain superior antitumor performance.

Despite the many advantages of fullerenes, their clinical application is still in its infancy, facing numerous challenges before their antitumor potential can be clinically exploited. Firstly, the structure of fullerene derivatives significantly affects their antitumor properties. Although various functional groups, amino acids, chromophores, etc. have been grafted on the surface of fullerenes, the specific effects of the modification positions and sizes of these groups on the performance of fullerene derivatives remain unclear. For example, in PDT, the relative position and distance between fullerenes and light-harvesting antennas affect phototransfer efficiency, influencing ROS production. The positions and quantities of hydroxyl groups in fullerlenols also greatly impact their antioxidative properties. Therefore, future research should delve deeper into the mechanisms to elucidate how the types, positions and sizes of groups influence the performance of fullerene derivatives.

Secondly, when using fullerene derivatives for PDT, it is crucial to consider the potential damage caused by ROS to normal tissue. To address this issue, it is essential to enhance the targeting and delivery efficiency of fullerene derivatives. Although various studies have modified fullerene surfaces with specific ligands to improve targetability, the interaction between fullerene derivatives and proteins in physiological environments must also be considered. Upon intravenous injection, only a small fraction of fullerene derivatives can reach the target area due to immune clearance.<sup>156</sup> When coming into contact with blood, serum proteins rapidly adsorb onto the surface of fullerene derivatives, forming protein coronas that interact with immune cells and promote phagocytosis. Additionally, adsorbed proteins may replace or cover the modified ligands or change their conformation, resulting in deteriorated targetability. Therefore, understanding the interactions between fullerene derivatives and serum proteins is essential for improving targetability and evading immune clearance. Future research should focus on designing novel fullerene derivatives capable of regulating protein corona formation.

Additionally, designing stimuli-responsive fullerene derivatives tailored to the tumor microenvironment can mitigate damage to normal tissue. For example, pH-responsive fullerene derivatives targeting the acidic tumor microenvironment or redox-responsive fullerene derivatives targeting the high-level glutathione within tumor cells can be developed. Incorporating triplet state switches may also ensure that fullerene derivatives generate significant amounts of ROS and  $^1\text{O}_2$  only within the tumor environment, thereby reducing harm to normal tissue.

Although fullerene derivatives show promise as emerging antitumor nanomaterials, they share common issues with other nanoparticles applied in cancer treatment. The biological safety of fullerene derivatives requires further validation. Some studies suggest that remnant fullerenes in the liver remained over 90% even after 168 h following intravenous injection into rats.<sup>8</sup> Before further clinical application, the comprehensive evaluation of the tissue toxicity of fullerene derivatives is necessary, and additional clinical data are needed to validate their biological safety.

To conclude, this review provides an overview of the commonly available fullerene derivatives for tumor treatment and their fundamental antitumor mechanisms, while also demonstrating some limitations. Future research should focus on the molecular design of fullerene derivatives, the development of stimuli-responsive fullerene derivatives tailored to the tumor microenvironment, the interactions between fullerene derivatives and serum proteins, as well as their tissue distribution and biosafety. Addressing these issues will facilitate the development of fullerene derivatives that can be clinically applied in tumor therapy.

## Acknowledgments

Wenjia Hou and Lan Shen are co-first authors for this study. Special thanks to Mr. Songze Wu for suggestions and language polishing. Graphical abstract is created in BioRender. Yang, F. (2024) BioRender.com/x74o589.

## Funding

This work was supported by the Natural Science Foundation of Zhejiang Province (grant # LQ21C100001), the State Key Laboratory of Molecular Engineering of Polymers (Fudan University) (grant # K2023-07), the National Natural Science Foundation of China (grant #32201139), and National 111 Project of China (grant # D16013).

## Disclosure

The authors declare no conflicts of interest in this work.

## References

1. Tang J, Pearce L, O'Donnell-Tormey J, Hubbard-Lucey VM. Trends in the global immuno-oncology landscape. *Nat Rev Drug Discov*. 2018;17(11):783–784. doi:10.1038/nrd.2018.202
2. Li M, Chen F, Yang Q, et al. Biomaterial-based CRISPR/Cas9 delivery systems for tumor treatment. *Biomater Res*. 2024;28:0023. doi:10.34133/bmr.0023
3. Jin HR, Yang Q, Wang FY, et al. Exploring tumor organoids for cancer treatment. *MPL Mater*. 2024;12:060602. doi:10.1063/5.0216185
4. Yang Q, Li S, Ou H, et al. Exosome-based delivery strategies for tumor therapy: an update on modification, loading, and clinical application. *J Nanobiotechnol*. 2024;22(1):41. doi:10.1186/s12951-024-02298-7
5. Ashrafzadeh M, Zarrabi A, Bigham A, et al. Nano)platforms in breast cancer therapy: drug/gene delivery, advanced nanocarriers and immunotherapy. *Med Res Rev*. 2023;43(6):2115–2176. doi:10.1002/med.21971
6. Huang P, Tang Q, Li M, et al. Manganese-derived biomaterials for tumor diagnosis and therapy. *J Nanobiotechnol*. 2024;22(1):335. doi:10.1186/s12951-024-02629-8
7. Amaral SI, Costa-Almeida R, Gonçalves IC, Magalhaes FD, Pinto AM. Carbon nanomaterials for phototherapy of cancer and microbial infections. *Carbon*. 2022;190:194–244. doi:10.1016/j.carbon.2021.12.084
8. Kazemzadeh H, Mozafari M. Fullerene-based delivery systems. *Drug Discovery Today*. 2019;24(3):898–905. doi:10.1016/j.drudis.2019.01.013
9. Krätschmer W, Lamb LD, Fostiropoulos K, Huffman DR. Solid C<sub>60</sub>: a new form of carbon. *Nature*. 1990;347(6291):354–358. doi:10.1038/347354a0
10. Ye L, Kollie L, Liu X, et al. Antitumor activity and potential mechanism of novel fullerene derivative nanoparticles. *Molecules*. 2021;26(11):3252. doi:10.3390/molecules26113252
11. Kroto HW, Heath JR, O'Brien SC, Curl RF, Smalley RE. C<sub>60</sub>: buckminsterfullerene. *Nature*. 1985;318(6042):162–163. doi:10.1038/318162a0
12. Nakamura S, Mashino T. Water-soluble fullerene derivatives for drug discovery. *J Nippon Med School*. 2012;79(4):248–254. doi:10.1272/jnms.79.248
13. Cui R, Li J, Huang H, et al. Novel carbon nano)hybrids as highly efficient magnetic resonance imaging contrast agents. *Nano Res*. 2015;8(4):1259–1268. doi:10.1007/s12274-014-0613-x
14. Kokubo K, Shirakawa S, Kobayashi N, Aoshima H, Oshima T. Facile and scalable synthesis of a highly hydroxylated water-soluble fullerene as a single nanoparticle. *Nano Res*. 2011;4(2):204–215. doi:10.1007/s12274-010-0071-z
15. Huang YY, Sharma SK, Yin R, Agrawal T, Chiang LY, Hamblin MR. Functionalized fullerenes in photodynamic therapy. *J Biomed Nanotechnol*. 2014;10(9):1918–1936. doi:10.1166/jbn.2014.1963
16. Li Q, Hong L, Li HG, Liu CG. Graphene oxide-fullerene C<sub>60</sub> (GO-C<sub>60</sub>) hybrid for photodynamic and photothermal therapy triggered by near-infrared light. *Biosens Bioelectron*. 2017;89:477–482. doi:10.1016/j.bios.2016.03.072
17. Deng RJ, Wang YQ, Zhen MM, et al. Real-time monitoring of tumor vascular disruption induced by radiofrequency assisted gadofullerene. *Sci China*. 2018;61(8):1101–1111. doi:10.1007/s40843-017-9223-6
18. Zhen MM, Shu CY, Li J, et al. A highly efficient and tumor vascular-targeting therapeutic technique with size-expandable gadofullerene nanocrystals. *Sci China*. 2015;58(10):799–810. doi:10.1007/s40843-015-0089-3
19. Prylutka S, Panchuk R, Golinski G, et al. C<sub>60</sub> fullerene enhances cisplatin anticancer activity and overcomes tumor cell drug resistance. *Nano Res*. 2017;10(2):652–671. doi:10.1007/s12274-016-1324-2
20. Li J, Chen L, Yan L, et al. A novel drug design strategy: an inspiration from encaging tumor by metallofullerene Gd@C<sub>(82)</sub>(OH)<sub>(22)</sub>. *Molecules*. 2019;24. doi:10.3390/molecules24132387
21. Fernandes NB, Shenoy RUK, Kajampady MK, et al. Fullerenes for the treatment of cancer: an emerging tool. *Environ Sci Pollut Res*. 2022;29(39):58607–58627. doi:10.1007/s11356-022-21449-7
22. Yang BW, Chen Y, Shi JL. Reactive oxygen species (ROS)-based nanomedicine. *Chem Rev*. 2019;119(8):4881–4985. doi:10.1021/acs.chemrev.8b00626
23. Markovic Z, Trajkovic V. Biomedical potential of the reactive oxygen species generation and quenching by fullerenes (C<sub>60</sub>). *Biomaterials*. 2008;29(26):3561–3573. doi:10.1016/j.biomaterials.2008.05.005
24. Isakovic A, Markovic Z, Todorovic-Markovic B, et al. Distinct cytotoxic mechanisms of pristine versus hydroxylated fullerene. *Toxicol Sci*. 2006;91(1):173–183. doi:10.1093/toxsci/kfj127
25. Abrahamse H, Hamblin MR. New photosensitizers for photodynamic therapy. *Biochem J*. 2016;473(4):347–364. doi:10.1042/bj20150942
26. Castano AP, Demidova TN, Hamblin MR. Mechanisms in photodynamic therapy: part one-photosensitizers, photochemistry and cellular localization. *Photodiagn Photodyn Ther*. 2004;1(4):279–293. doi:10.1016/s1572-1000(05)00007-4
27. Henderson BW, Dougherty TJ. How does photodynamic therapy work? *Photochem Photobiol*. 1992;55(1):145–157. doi:10.1111/j.1751-1097.1992.tb04222.x
28. Agostinis P, Berg K, Cengel KA, et al. Photodynamic therapy of cancer: an update. *CA Cancer J Clin*. 2011;61(4):250–281. doi:10.3322/caac.20114
29. Hanahan D, Weinberg RA. Hallmarks of cancer: the next generation. *Cell*. 2011;144:646–674. doi:10.1016/j.cell.2011.02.013
30. Dolmans D, Fukumura D, Jain RK. Photodynamic therapy for cancer. *Nat Rev Cancer*. 2003;3(5):380–387. doi:10.1038/nrc1071
31. Dong YX, Cao W, Cao J. Treatment of rheumatoid arthritis by phototherapy: advances and perspectives. *Nanoscale*. 2021;13(35):14591–14608. doi:10.1039/d1nr03623h
32. Krusic PJ, Wasserman E, Keizer PN, Morton JR, Preston KF. Radical Reactions of C<sub>60</sub>. *Science*. 1991;254(5035):1183–1185. doi:10.1126/science.254.5035.1183
33. Sharma SK, Chiang LY, Hamblin MR. Photodynamic Therapy with Fullerenes in vivo: reality or a Dream? *Nanomedicine*. 2011;6(10):1813–1825. doi:10.2217/nmm.11.144
34. Foley S, Crowley C, Smahli M, et al. Cellular localisation of a water-soluble fullerene derivative. *Biochem Biophys Res Commun*. 2002;294(1):116–119. doi:10.1016/S0006-291X(02)00445-X
35. Nishizawa C, Hashimoto N, Yokoo S, et al. Pyrrolidinium-type fullerene derivative-induced apoptosis by the generation of reactive oxygen species in HL-60 cells. *Free Rad Res*. 2009;43(12):1240–1247. doi:10.3109/10715760903273849

36. Palyvoda KO, Grynyuk II, Prylutska SV, Samoylenko AA, Drobot LB, Matyshevska OP; PMID: 21513214. Apoptosis photoinduction by C<sub>60</sub> fullerene in human leukemic T cells. *Ukrain Biochem J.* 1999;82(2010):121–127.
37. Rancan F, Rosan S, Boehm F, et al. Cytotoxicity and photocytotoxicity of a dendritic C(60) mono-adduct and a malonic acid C(60) tris-adduct on Jurkat cells. *J Photochem Photobiol B.* 2002;67(3):157–162. doi:10.1016/s1011-1344(02)00320-2
38. Shi J, Wang Z, Wang L, et al. Photodynamic therapy of a 2-methoxyestradiol tumor-targeting drug delivery system mediated by Asn-Gly-Arg in breast cancer. *Int J Nanomed.* 2013;8:1551–1562. doi:10.2147/ijn.S40011
39. Oleinick NL, Morris RL, Belichenko T. The role of apoptosis in response to photodynamic therapy: what, where, why, and how. *Photochem Photobiol Sci.* 2002;1(1):1–21. doi:10.1039/b108586g
40. Yanga LY, Gaob JL, Gaoa T, et al. Toxicity of polyhydroxylated fullerene to mitochondria. *J Hazard Mater.* 2016;301:119–126. doi:10.1016/j.jhazmat.2015.08.046
41. Lowe SW, Lin AW. Apoptosis in cancer. *Carcinogenesis.* 2000;21(3):485–495. doi:10.1093/carcin/21.3.485
42. Czabotar PE, Garcia-Saez AJ. Mechanisms of BCL-2 family proteins in mitochondrial apoptosis. *Nat Rev Mol Cell Biol.* 2023;24(10):732–748. doi:10.1038/s41580-023-00629-4
43. Park H, Kam T, Dawson TM, Dawson VL. Poly (ADP-ribose) (PAR)-dependent cell death in neurodegenerative diseases. *Int Rev Cell Mol Biol.* 2020;353:1–29. doi:10.1016/bs.iremb.2019.12.009
44. Mroz P, Pawlak A, Satti M, et al. Functionalized fullerenes mediate photodynamic killing of cancer cells: type I versus Type II photochemical mechanism. *Free Rad Biol Med.* 2007;43(5):711–719. doi:10.1016/j.freeradbiomed.2007.05.005
45. Susin SA, Lorenzo HK, Zamzami N, et al. Molecular characterization of mitochondrial apoptosis-inducing factor. *Nature.* 1999;397(6718):441–446. doi:10.1038/17135
46. Arnoult D. Mitochondrial release of AIF and EndoG requires caspase activation downstream of Bax/Bak-mediated permeabilization. *THE EMBO Journal.* 2003;22(17):4385–4399. doi:10.1093/emboj/cdg423
47. Sayes CM, Gobin AM, Ausman KD, Mendez J, West JL, Colvin VL. Nano-C<sub>60</sub> cytotoxicity is due to lipid peroxidation. *Biomaterials.* 2005;26(36):7587–7595. doi:10.1016/j.biomaterials.2005.05.027
48. Sera N, Tokiwa H, Miyata N. Mutagenicity of the fullerene C<sub>60</sub> -generated singlet oxygen dependent formation of lipid peroxides. *Carcinogenesis.* 1996;17(10):2163–2169. doi:10.1093/carcin/17.10.2163
49. Kamat JP, Devasagayam TP, Priyadarsini KI, Mohan H. Reactive oxygen species mediated membrane damage induced by fullerene derivatives and its possible biological implications. *Toxicology.* 2000;155(1–3):55–61. doi:10.1016/s0300-483x(00)00277-8
50. Suhail Y, Cain MP, Vanaja K, et al. Systems Biology of Cancer Metastasis. *Cell Systems.* 2019;9(2):109–127. doi:10.1016/j.cels.2019.07.003
51. Qin Y, Chen K, Gu W, et al. Small size fullerene nanoparticles suppress lung metastasis of breast cancer cell by disrupting actin dynamics. *J Nanobiotechnol.* 2018;16(1). doi:10.1186/s12951-018-0380-z
52. Conlon GA, Murray GI. Recent advances in understanding the roles of matrix metalloproteinases in tumour invasion and metastasis. *J Pathol.* 2019;247(5):629–640. doi:10.1002/path.5225
53. Deryugina EI, Quigley JP. Matrix metalloproteinases and tumor metastasis. *Cancer Metastasis Rev.* 2006;25(1):9–34. doi:10.1007/s10555-006-7886-9
54. Merchant N, Nagaraju GP, Rajitha B, et al. Matrix metalloproteinases: their functional role in lung cancer. *Carcinogenesis.* 2017;38(8):766–780. doi:10.1093/carcin/bgx063
55. Liu J, Kang SG, Wang P, et al. Molecular mechanism of Gd@C<sub>82</sub>(OH)<sub>22</sub> increasing collagen expression: implication for encaging tumor. *Biomaterials.* 2018;152:24–36. doi:10.1016/j.biomaterials.2017.10.027
56. Nie X, Tang J, Liu Y, et al. Fullerenol inhibits the cross-talk between bone marrow-derived mesenchymal stem cells and tumor cells by regulating MAPK signaling. *Nanomedicine.* 2017;13(6):1879–1890. doi:10.1016/j.nano.2017.03.013
57. Valcourt DM, Harris J, Riley RS, Dang M, Wang JX, Day ES. Advances in targeted nanotherapeutics: from bioconjugation to biomimicry. *Nano Res.* 2018;11(10):4999–5016. doi:10.1007/s12274-018-2083-z
58. Qi CX, Liu XS, Zhi DK, et al. Exosome-mimicking nanovesicles derived from efficacy-potentiated stem cell membrane and secretome for regeneration of injured tissue. *Nano Res.* 2022;15(2):1680–1690. doi:10.1007/s12274-021-3868-z
59. Dongre A, Weinberg RA. New insights into the mechanisms of epithelial-mesenchymal transition and implications for cancer. *Nat Rev Mol Cell Biol.* 2019;20(2):69–84. doi:10.1038/s41580-018-0080-4
60. Altorki NK, Markowitz GJ, Gao D, et al. The lung microenvironment: an important regulator of tumor growth and metastasis. *Nat Rev Cancer.* 2019;19(1):9–31. doi:10.1038/s41568-018-0081-9
61. Lin Y, Xu J, Lan H. Tumor-associated macrophages in tumor metastasis: biological roles and clinical therapeutic applications. *J Hematol Oncol.* 2019;12(1):76. doi:10.1186/s13045-019-0760-3
62. Saitoh M. Involvement of partial EMT in cancer progression. *Journal of Biochemistry.* 2018;164(4):257–264. doi:10.1093/jb/mvy047
63. Zhou W, Huo JW, Yang Y, et al. Aminated fullerene abrogates cancer cell migration by directly targeting myosin heavy chain 9. *ACS Appl Mater Interfaces.* 2020;12(51):56862–56873. doi:10.1021/acsami.0c18785
64. Emprou C, Le Van Quyen P, Jégu J, et al. SNAI 2 and TWIST 1 in lymph node progression in early stages of NSCLC patients. *Cancer Med.* 2018;7(7):3278–3291. doi:10.1002/cam4.1545
65. Horak I, Prylutska S, Krysiuk I, et al. Nanocomplex of berberine with C<sub>60</sub> fullerene is a potent suppressor of Lewis Lung carcinoma cells invasion *in vitro* and metastatic activity *in vivo*. *Materials.* 2021;14(20):6114. doi:10.3390/ma14206114
66. Yang L, Yang X, Ji W, et al. Effects of a Functional Variant c.353T>C in Snai1 on Risk of Two Contextual Diseases. Chronic Obstructive Pulmonary Disease and Lung Cancer. *Am J Respir Critical Care Med.* 2014;189(2):139–148. doi:10.1164/rccm.201307-1355OC
67. Liao Y, Wang C, Yang Z, et al. Dysregulated Sp1/miR-130b-3p/HOXA5 axis contributes to tumor angiogenesis and progression of hepatocellular carcinoma. *Theranostics.* 2020;10(12):5209–5224. doi:10.7150/thno.43640
68. Petrillo M, Patella F, Pesapane F, et al. Hypoxia and tumor angiogenesis in the era of hepatocellular carcinoma transarterial loco-regional treatments. *Future Oncol.* 2018;14(28):2957–2967. doi:10.2217/fon-2017-0739
69. Cubillos-Ruiz JR, Bettigole SE, Glimcher LH. Tumorigenic and immunosuppressive effects of endoplasmic reticulum stress in cancer. *Cell.* 2017;168(4):692–706. doi:10.1016/j.cell.2016.12.004



70. Zhou Y, Zhen M, Guan M, et al. Amino acid modified fullerene derivatives with high radical scavenging activity as promising bodyguards for chemotherapy protection. *Sci Rep*. 2018;8(1):16573. doi:10.1038/s41598-018-34967-7
71. Guan M, Zhou Y, Liu S, et al. Photo-triggered gadofullerene: enhanced cancer therapy by combining tumor vascular disruption and stimulation of anti-tumor immune responses. *Biomaterials*. 2019;213:119218. doi:10.1016/j.biomaterials.2019.05.029
72. Folkman J, Parris EE, Folkman J. Tumor angiogenesis: therapeutic implications. *New Engl J Med*. 1971;285(21):1182–1186. doi:10.1056/NEJM197111182852108
73. Hashizume H, Baluk P, Morikawa S, et al. Openings between defective endothelial cells explain tumor vessel leakiness. *Am J Pathol*. 2000;156(4):1363–1380. doi:10.1016/s0002-9440(10)65006-7
74. Prylutka S, Grynyuk I, Skaterna T, et al. Toxicity of C<sub>60</sub> fullerene–cisplatin nanocomplex against Lewis lung carcinoma cells. *Arch Toxicol*. 2019;93(5):1213–1226. doi:10.1007/s00204-019-02441-6
75. Chen C, Xing G, Wang J, et al. Multihydroxylated [Gd@C<sub>82</sub>(OH)<sub>22</sub>] n Nanoparticles: antineoplastic Activity of High Efficiency and Low Toxicity. *Nano Lett*. 2005;5(10):2050–2057. doi:10.1021/nl051624b
76. Li YY, Tian YH, Nie GJ. Antineoplastic activities of Gd@C<sub>82</sub>(OH)<sub>22</sub> nanoparticles: tumor microenvironment regulation. *Sci China*. 2012;55(10):884–890. doi:10.1007/s11427-012-4387-7
77. Liu Y, Jiao F, Qiu Y, et al. The effect of Gd@C<sub>82</sub>(OH)<sub>22</sub> nanoparticles on the release of Th1/Th2 cytokines and induction of TNF-alpha mediated cellular immunity. *Biomaterials*. 2009;30(23–24):3934–3945. doi:10.1016/j.biomaterials.2009.04.001
78. Grebowski J, Litwinienko G. Metallofullerenols in biomedical applications. *Eur J Med Chem*. 2022;238:114481. doi:10.1016/j.ejmech.2022.114481
79. Sanmamed MF, Chen L. A paradigm shift in cancer immunotherapy: from enhancement to normalization. *Cell*. 2018;175(2):313–326. doi:10.1016/j.cell.2018.09.035
80. Hirschhorn D, Budhu S, Kraehenbuehl L, et al. T cell immunotherapies engage neutrophils to eliminate tumor antigen escape variants. *Cell*. 2023;186(7):1432–1447.e1417. doi:10.1016/j.cell.2023.03.007
81. Lang F, Schrörs B, Löwer M, Türeci Ö, Sahin U. Identification of neoantigens for individualized therapeutic cancer vaccines. *Nat Rev Drug Discov*. 2022;21(4):261–282. doi:10.1038/s41573-021-00387-y
82. Leko V, Rosenberg SA. Identifying and targeting human tumor antigens for T cell-based immunotherapy of solid tumors. *Cancer Cell*. 2020;38(4):454–472. doi:10.1016/j.ccell.2020.07.013
83. Takeuchi A, Saito T. CD4 CTL, a cytotoxic subset of CD4(+) T cells, their differentiation and function. *Front Immunol*. 2017;8:194. doi:10.3389/fimmu.2017.00194
84. Yang D, Zhao YL, Guo H, et al. [[Gd@C<sub>82</sub>(OH)<sub>22</sub>]n Nanoparticles Induce Dendritic Cell Maturation and Activate Th1 Immune Responses. *ACS Nano*. 2010;4(2):1178–1186. doi:10.1021/nn901478z
85. Martinez FO, Sica A, Mantovani A, Locati M. Macrophage activation and polarization. *Front Biosci*. 2008;13(13):453–461. doi:10.2741/2692
86. Fagone P, Di Rosa M, Palumbo M, De Gregorio C, Nicoletti F, Malaguarnera L. Modulation of heat shock proteins during macrophage differentiation. *Inflammation Res*. 2012;61(10):1131–1139. doi:10.1007/s00011-012-0506-y
87. Sica A, Mantovani A. Macrophage plasticity and polarization: in vivo veritas. *J Clin Invest*. 2012;122(3):787–795. doi:10.1172/jci59643
88. Chen K, Wang YJ, Liang HJ, et al. Fullerenols boosting the therapeutic effect of anti-CD47 antibody to trigger robust anti-tumor immunity by inducing calreticulin exposure. *Nano Today*. 2021;37:101070. doi:10.1016/j.nantod.2020.101070
89. Li L, Zhen MM, Wang HY, et al. Functional Gadofullerene nanoparticles trigger robust cancer immunotherapy based on rebuilding an immunosuppressive tumor microenvironment. *Nano Lett*. 2020;20(6):4487–4496. doi:10.1021/acs.nanolett.0c01287
90. Chiang LY, Padmawar PA, Rogers-Haley JE, et al. Synthesis and characterization of highly photoresponsive fullerene dyads with a close chromophore antenna–C<sub>60</sub> contact and effective photodynamic potential. *J Mater Chem*. 2010;20(25):5280–5293. doi:10.1039/c0jm00037j
91. Liu X, Zheng M, Kong X, et al. Separately doped upconversion-C<sub>60</sub> nanoplatfrom for NIR imaging-guided photodynamic therapy of cancer cells. *Chem Commun*. 2013;49(31):3224–3226. doi:10.1039/c3cc41013g
92. Du B, Han S, Zhao F, et al. A smart upconversion-based light-triggered polymer for synergetic chemo-photodynamic therapy and dual-modal MR/UCL imaging. *Nanomedicine*. 2016;12(7):2071–2080. doi:10.1016/j.nano.2016.05.004
93. Shi H, Gu R, Xu W, et al. Near-Infrared light-harvesting fullerene-based nanoparticles for promoted synergetic tumor phototheranostics. *ACS Appl Mater Interfaces*. 2019;11(48):44970–44977. doi:10.1021/acsami.9b17716
94. Guo W, Liu X, Ye LJ, et al. The effect of polyhydroxy fullerene derivative on human myeloid Leukemia K562 cells. *Materials*. 2022;15:1349. doi:10.3390/ma15041349
95. Jiao F, Liu Y, Qu Y, et al. Studies on anti-tumor and antimetastatic activities of fullereneol in a mouse breast cancer model. *Carbon*. 2010;48(8):2231–2243. doi:10.1016/j.carbon.2010.02.032
96. Trajković S, Dobrić S, Jačević V, Dragojević-Simić V, Milovanović Z, Dorđević A. Tissue-protective effects of fullereneol C<sub>60</sub>(OH)<sub>24</sub> and amifostine in irradiated rats. *Colloids Surf B*. 2007;58(1):39–43. doi:10.1016/j.colsurfb.2007.01.005
97. Cai X, Hao J, Zhang X, et al. The polyhydroxylated fullerene derivative C<sub>60</sub>(OH)<sub>24</sub> protects mice from ionizing-radiation-induced immune and mitochondrial dysfunction. *Toxicol Appl Pharmacol*. 2010;243(1):27–34. doi:10.1016/j.taap.2009.11.009
98. Injac R, Perse M, Obermajer N, et al. Potential hepatoprotective effects of fullereneol C<sub>60</sub>(OH)<sub>24</sub> in doxorubicin-induced hepatotoxicity in rats with mammary carcinomas. *Biomaterials*. 2008;29(24–25):3451–3460. doi:10.1016/j.biomaterials.2008.04.048
99. Chaudhuri P, Paraskar A, Soni S, Mashelkar RA, Sengupta S. Fullereneol-cytotoxic conjugates for cancer chemotherapy. *ACS Nano*. 2009;3(9):2505–2514. doi:10.1021/nn900318y
100. Jovic DS, Seke MN, Djordjevic AN, et al. Fullereneol nanoparticles as a new delivery system for doxorubicin. *RSC Adv*. 2016;6(45):38563–38578. doi:10.1039/c6ra03879d
101. Meng H, Xing G, Blanco E, et al. Gadolinium metallofullerene nanoparticles inhibit cancer metastasis through matrix metalloproteinase inhibition: imprisoning instead of poisoning cancer cells. *Nanomedicine*. 2012;8(2):136–146. doi:10.1016/j.nano.2011.08.019
102. Kang SG, Zhou G, Yang P, et al. Molecular mechanism of pancreatic tumor metastasis inhibition by Gd@C<sub>82</sub>(OH)<sub>22</sub> and its implication for de novo design of nanomedicine. *Proc Natl Acad Sci USA*, 109 (2012) 15431–15436. doi:10.1073/pnas.1204600109
103. Yin X, Zhao L, Kang SG, et al. Impacts of fullerene derivatives on regulating the structure and assembly of collagen molecules. *Nanoscale*. 2013;5(16):7341–7348. doi:10.1039/c3nr01469j

104. Pan Y, Wang L, Kang SG, et al. Gd-metallofullerenol nanomaterial suppresses pancreatic cancer metastasis by inhibiting the interaction of histone deacetylase 1 and metastasis-associated protein 1. *ACS Nano*. 2015;9(7):6826–6836. doi:10.1021/nn506782f
105. Ren JY, Cai R, Wang J, et al. Precision nanomedicine development based on specific opsonization of human cancer patient-personalized protein coronas. *Nano Lett*. 2019;19(7):4692–4701. doi:10.1021/acs.nanolett.9b01774
106. Lu Z, Jia W, Deng R, et al. Light-assisted gadofullerene nanoparticles disrupt tumor vasculatures for potent melanoma treatment. *J Mat Chem B*. 2020;8(12):2508–2518. doi:10.1039/c9tb02752a
107. Li Z, Pan LL, Zhang FL, Wang Z, Shen YY, Zhang ZZ. Preparation and characterization of fullerene (C<sub>60</sub>) amino acid nanoparticles for liver cancer cell treatment. *J Nanosci Nanotechnol*. 2014;14(6):4513–4518. doi:10.1166/jnn.2014.8242
108. Belik AY, Rybkin AY, Goryachev NS, et al. Nanoparticles of water-soluble dyads based on amino acid fullerene C(60) derivatives and pyrophosphoribide: synthesis, photophysical properties, and photodynamic activity, *Spectrochimica Acta Part A. Mol Biomol Spectrosc*. 2021;260:119885. doi:10.1016/j.saa.2021.119885
109. Barańska E, Wiecheć-Cudak O, Rak M, et al. Interactions of a Water-soluble glycofullerene with glucose transporter 1. Analysis of the cellular effects on a pancreatic tumor model. *Nanomaterials*. 2021;11(2):513. doi:10.3390/nano11020513
110. Korzuch J, Rak M, Balin K, et al. Towards water-soluble [60]fullerenes for the delivery of siRNA in a prostate cancer model. *Sci Rep*. 2021;11(1):10565. doi:10.1038/s41598-021-89943-5
111. Serda M, Ware MJ, Newton JM, et al. Development of Photoactive Sweet-C<sub>60</sub> for Pancreatic Cancer Stellate Cell Therapy. *Nanomedicine*. 2018;13(23):2981–2993. doi:10.2217/nnm-2018-0239
112. Agazzi ML, Almodovar VAS, Gsponer NS, Bertolotti S, Tomé AC, Durantini EN. Diketopyrrolopyrrole–fullerene C<sub>60</sub> architectures as highly efficient heavy atom-free photosensitizers: synthesis, photophysical properties and photodynamic activity. *Org Biomol Chem*. 2020;18(7):1449–1461. doi:10.1039/c9ob02487e
113. Sobotta L, Skupin-Mrugalska P, Piskorz J, Mielcarek J. Non-porphyrinoid photosensitizers mediated photodynamic inactivation against bacteria. *Dyes Pigm*. 2019;163:337–355. doi:10.1016/j.dyepig.2018.12.014
114. Juzeniene A, Nielsen KP, Moan J. Biophysical aspects of photodynamic therapy. *J Environ Pathol Toxicol Oncol*. 2006;25(1–2):7–28. doi:10.1615/JEnvironPatholToxicolOncol.v25.i1-2.20
115. Frangioni JV. in vivo near-infrared fluorescence imaging. *Curr Opin Chem Biol*. 2003;7(5):626–634. doi:10.1016/j.cbpa.2003.08.007
116. Del Valle CA, Hirsch T, Marin MJ. Recent advances in near infrared upconverting nanomaterials for targeted photodynamic therapy of cancer. *Method Appl Fluoresc*. 2022;10(3):034003. doi:10.1088/2050-6120/ac6937
117. Idris NM, Gnanasammandhan MK, Zhang J, Ho PC, Mahendran R, Zhang Y. in vivo photodynamic therapy using upconversion nanoparticles as remote-controlled nanotransducers. *Nat Med*. 2012;18(10):1580–U1190. doi:10.1038/nm.2933
118. Antoku D, Satake S, Mae T, et al. Improvement of photodynamic activity of lipid-membrane-incorporated fullerene derivative by combination with a photo-antenna molecule. *Chemistry*. 2018;24(29):7335–7339. doi:10.1002/chem.201800674
119. Tang Q, Xiao W, Li J, et al. A fullerene-rhodamine B photosensitizer with pH-activated visible-light absorbance/fluorescence/photodynamic therapy. *J Mater Chem B*. 2018;6(18):2778. doi:10.1039/c8tb00372f
120. Negri V, Pacheco-Torres J, Calle D, López-Larrubia P. Carbon nanotubes in biomedicine. *Top Current Chem*. 2020;378(1):15. doi:10.1007/s41061-019-0278-8
121. Grebowski J, Kazmierska P, Krokosz A. Fullerenols as a new therapeutic approach in nanomedicine. *Biomed Res Int*. 2013;2013:751913. doi:10.1155/2013/751913
122. Kovel ES, Sachkova AS, Vnukova NG, Churilov GN, Knyazeva EM, Kudryasheva NS. Antioxidant activity and toxicity of fullerenols via bioluminescence signaling: role of oxygen substituents. *Int J Mol Sci*. 2019;20(9):2324. doi:10.3390/ijms20092324
123. Nobre AR, Risson E, Singh DK, et al. Bone marrow NG2(+)/Nestin(+) mesenchymal stem cells drive DTC dormancy via TGFβ2. *Nat Cancer*. 2021;2(3):327–339. doi:10.1038/s43018-021-00179-8
124. Mirkov SM, Djordjevic AN, Andric NL, et al. Nitric oxide-scavenging activity of polyhydroxylated fullerene C<sub>60</sub>(OH)<sub>24</sub>. *Nitric Oxide-Biol Chem*. 2004;11(2):201–207. doi:10.1016/j.niox.2004.08.003
125. Prat F, Stackow R, Bernstein R, Qian WY, Rubin Y, Foote CS. Triplet-state properties and singlet oxygen generation in a homologous series of functionalized fullerene derivatives. *J Phys Chem A*. 1999;103(36):7230–7235. doi:10.1021/jp991237o
126. Grębowski J, Kaźmierska P, Krokosz A. Fullereneol - properties and applications in biomedical sciences. *Postepy Hig Med Dosw*. 2013;67:859–872. doi:10.5604/17322693.1063743
127. Lichota A, Krokosz A. Fullerenols in therapy and diagnosis of cancer. *Medycyna Pracy*. 2016;67(6):817–831. doi:10.13075/mp.5893.00466
128. Zhou Y, Li J, Ma H, et al. Biocompatible [60]/[70] fullerenols: potent defense against oxidative injury induced by reduplicative chemotherapy. *ACS Appl Mater Interfaces*. 2017;9(41):35539–35547. doi:10.1021/acsami.7b08348
129. Carvalho C, Santos RX, Cardoso S, et al. Doxorubicin: the good, the bad and the ugly effect. *Current Med Chem*. 2009;16(25):3267–3285. doi:10.2174/092986709788803312
130. Srdjenovic B, Milic-Torres V, Grujic N, Stankov K, Djordjevic A, Vasovic V. Antioxidant properties of fullerene C<sub>60</sub>(OH)<sub>24</sub> in rat kidneys, testes, and lungs treated with doxorubicin. *Toxicol Mech Methods*. 2010;20(6):298–305. doi:10.3109/15376516.2010.485622
131. Chao MP, Majeti R, Weissman IL. Programmed cell removal: a new obstacle in the road to developing cancer. *Nat Rev Cancer*. 2012;12(1):58–67. doi:10.1038/nrc3171
132. Pankhurst QA, Connolly J, Jones SK, Dobson J. Applications of magnetic nanoparticles in biomedicine. *J Phys D Appl Phys*. 2003;36(13):167–181. doi:10.1088/0022-3727/36/13/201
133. Liang XJ, Meng H, Wang Y, et al. Metallofullerene nanoparticles circumvent tumor resistance to cisplatin by reactivating endocytosis. *Proc Natl Acad Sci USA*. 2010;107(16):7449–7454. doi:10.1073/pnas.0909707107
134. Meng H, Xing G, Sun B, et al. Potent angiogenesis inhibition by the particulate form of fullerene derivatives. *ACS Nano*. 2010;4(5):2773–2783. doi:10.1021/nn100448z
135. Zhou Y, Deng R, Zhen M, et al. Amino acid functionalized gadofullerene nanoparticles with superior antitumor activity via destruction of tumor vasculature in vivo. *Biomaterials*. 2017;133:107–118. doi:10.1016/j.biomaterials.2017.04.025
136. Tang J, Chen Z, Sun B, et al. Polyhydroxylated fullerenols regulate macrophage for cancer adoptive immunotherapy and greatly inhibit the tumor metastasis. *Nanomedicine*. 2016;12(4):945–954. doi:10.1016/j.nano.2015.11.021

137. Chen SH, Kang S, Luo J, Zhou R. Charging nanoparticles: increased binding of Gd@C 82 (OH) 22 derivatives to human MMP-9. *Nanoscale*. 2018;10(12):5667–5677. doi:10.1039/c8nr00127h
138. Li X, Zhen M, Deng R, et al. RF-assisted gadofullerene nanoparticles induces rapid tumor vascular disruption by down-expression of tumor vascular endothelial cadherin. *Biomaterials*. 2018;163:142–153. doi:10.1016/j.biomaterials.2018.02.028
139. Lühr JJ, Alex N, Amon L, et al. Maturation of monocyte-derived DCs leads to increased cellular stiffness, higher membrane fluidity, and changed lipid composition. *Front Immunol*. 2020;11:590121. doi:10.3389/fimmu.2020.590121
140. Mbongue JC, Nieves HA, Torrez TW, Langridge WH. The role of dendritic cell maturation in the induction of insulin-dependent diabetes mellitus. *Front Immunol*. 2017;8:327. doi:10.3389/fimmu.2017.00327
141. Wang S, Zhou Z, Wang Z, et al. Gadolinium metallofullerene-based activatable contrast agent for tumor signal amplification and monitoring of drug release. *Small*. 2019;15(16):e1900691. doi:10.1002/smll.201900691
142. Rouse JG, Yang JZ, Barron AR, Monteiro-Riviere NA. Fullerene-based amino acid nanoparticle interactions with human epidermal keratinocytes. *Toxicol In Vitro*. 2006;20(8):1313–1320. doi:10.1016/j.tiv.2006.04.004
143. Da Ros T, Prato M. Medicinal chemistry with fullerenes and fullerene derivatives. *Chem Commun*. 1999;8(8):663–669. doi:10.1039/A809495K
144. Yang XL, Ebrahimi A, Li J, Cui QJ. Fullerene-biomolecule conjugates and their biomedical applications. *Int J Nanomed*. 2014;9:77–92. doi:10.2147/ijn.S52829
145. Nalepa P, Gawecki R, Szewczyk G, et al. A [60]fullerene nanoconjugate with gemcitabine: synthesis, biophysical properties and biological evaluation for treating pancreatic cancer. *Cancer Nanotechnol*. 2020;11(1):2. doi:10.1186/s12645-020-00058-4
146. Serda M, Gawecki R, Dulski M, et al. Synthesis and applications of [60] fullerene nanoconjugate with 5-aminolevulinic acid and its glycoconjugate as drug delivery vehicles. *R Soc Chem Adv*. 2022;12(11):6377. doi:10.1039/d1ra08499b
147. Li L, Bai C, Bai C, et al. Developing hypoxia-sensitive system via designing tumor-targeted fullerene-based photosensitizer for multimodal therapy of deep Tumor. *Adv Mater*. 2024;36(23):e2310875. doi:10.1002/adma.202310875
148. Malarz K, Korzuch J, Marforio TD, et al. Identification and biological evaluation of a water-soluble fullerene nanomaterial as BTK kinase inhibitor. *Int J Nanomed*. 2023;18:1709–1724. doi:10.2147/IJN.S403058
149. Di Giosia M, Bomans PHH, Bottoni A, et al. Proteins as supramolecular hosts for C<sub>60</sub>: a true solution of C<sub>60</sub> in water. *Nanoscale*. 2018;10(21):9908. doi:10.1039/C8NR02220H
150. Giosia MD, Soldà A, Seeger M, et al. A bio-conjugated fullerene as a subcellular-targeted and multifaceted phototheranostic agent. *Adv Funct Mater*. 2021;31(20):2101527. doi:10.1002/adfm.202101527
151. Heiden MG, Cantley LC, Thompson CB. Understanding the Warburg effect: the metabolic requirements of cell proliferation. *Science*. 2009;324(5930):1029–1033. doi:10.1126/science.1160809
152. Elstrom RL, Bauer DE, Buzzai M, et al. Akt stimulates aerobic glycolysis in cancer cells. *Cancer Res*. 2004;64(11):3892–3899. doi:10.1158/0008-5472.Can-03-2904
153. Wang J, Ye CY, Chen C, et al. Glucose transporter GLUT1 expression and clinical outcome in solid tumors: a systematic review and meta-analysis. *Oncotarget*. 2017;8(10):16875–16886. doi:10.18632/oncotarget.15171
154. Serda M, Malarz K, Mrozek-Wilczkiewicz A, Wojtyniak M, Musiol R, Curley SA. Glycofullerenes as non-receptor tyrosine kinase inhibitors-towards better nanotherapeutics for pancreatic cancer treatment. *Sci Rep*. 2020;10(1). doi:10.1038/s41598-019-57155-7
155. Wang H, Li L, Cao X, et al. Application of mannose-modified fullerene immunomodulator selectively polarizes tumor-associated macrophages potentiating antitumor immunity. *Nano Res*. 2023;16:12855–12863. doi:10.1007/s12274-023-6266-x
156. Shipkowski KA, Sanders JM, McDonald JD, Walker NJ, Waidyanatha S. Disposition of fullerene C<sub>60</sub> in rats following intratracheal or intravenous administration. *Xenobiotica*. 2019;49(9):1078–1085. doi:10.1080/00498254.2018.1528646